REVIEW ARTICLE

# The search for novel, superhard materials

Stan Vepřek[a)]
*Institute for Chemistry of Inorganic Materials, Technical University Munich, Lichtenbergstrasse 4, D-85747 Garching b. Munich, Germany*

(Received 1 January 1999; accepted 16 March 1999)

The recent development in the field of superhard materials with Vickers hardness of $\geqslant$40 GPa is reviewed. Two basic approaches are outlined including the intrinsic superhard materials, such as diamond, cubic boron nitride, $C_3N_4$, carbonitrides, etc. and extrinsic, nanostructured materials for which superhardness is achieved by an appropriate design of their microstructure. The theoretically predicted high hardness of $C_3N_4$ has not been experimentally documented so far. Ceramics made of cubic boron nitride prepared at high pressure and temperature find many applications whereas thin films prepared by activated deposition from the gas phase are still in the stage of fundamental development. The greatest progress has been achieved in the field of nanostructured materials including superlattices and nanocomposites where superhardness of $\geqslant$50 GPa was reported for several systems. More recently, *nc*-TiN/$SiN_x$ nanocomposites with hardness of 105 GPa were prepared, reaching the hardness of diamond. The principles of design for these materials are summarized and some unresolved questions outlined.  [S0734-2101(99)02205-8]

## I. INTRODUCTION

Figure 1 shows the Vickers hardness of selected hard materials including the heterostructures and nanocrystalline composites (''nanocomposites'') to be discussed in this review. By definition, ''superhard'' means materials whose Vickers hardness, $H_V$, exceeds 40 GPa. The search for superhard materials is driven by both the scientific curiosity of researchers to explore the possibilities of synthesizing a material whose hardness could approach or even exceed that of diamond and the technical importance of hard and superhard materials for wear protection of, e.g., machining tools. In most of the machining applications, hardness is only one of many other properties, such as high hot hardness and toughness (up to $\geqslant$800 °C), oxidation resistance, chemical stability and a low coefficient of friction against the material to be machined, high adherence, and compatibility with the substrate and low thermal conductivity, which such a material has to meet.[1,2] The importance of hard wear protective coatings for the machining application is illustrated by the fact that today more than 40% of all cutting tools are coated by wear resistant coatings and the market is growing fast. Wear resistant, superhard coatings for high speed dry machining would allow the industry to increase the productivity of expensive automated machines and to save on the high costs presently needed for environmentally hazardous coolants. Depending on the kind of machining, the recycling costs of these coolants amount to 10%–40% of the total machining costs. For example, in Germany alone these costs approach one billion $ U.S. per year.[3]

Superhard materials can be divided into intrinsic, such as diamond ($H_V \approx 70-100$ GPa), cubic boron nitride (*c*-BN, $H_V \approx 48$ GPa) and possibly some ternary compounds from the B–N–C triangle,[4] and extrinsic, whose superhardness and other mechanical properties are determined by their microstructure. The example par excellence for the latter class (extrinsic) of superhard materials is heterostructures (''superlattices''), artificial, man-made periodic arrangements of epitaxial, several nanometer thin layers of two different materials as originally suggested by Koehler[5] and later on extended to polycrystalline heterostructures. More recently, nanocrystalline (*nc*) composites, such as *nc*-$M_nN$/*a*-$Si_3N_4$ (M)=Ti,W,V and other hard transition metal nitrides, *a*-$Si_3N_4$ being an amorphous silicon nitride), *nc*-TiN/BN, *nc*-TiN/ $TiB_2$, and others were developed whose hardness exceeds 50 GPa, and in the case of *nc*-TiN/$SiN_x$ reaches 105 GPa. Because of the large variety of possible material combinations that yield superhardness, superhard nanocomposites hold the best promise of meeting all the complex demands on technically applicable superhard materials.

The remarkable property of nanostructured superhard materials is the fact that their hardness significantly exceeds that given by the rule of mixture. According to the ''rule of mixture,'' the hardness of a mixture $H(A_aB_b)=[a\cdot H(A)+b\cdot H(B)]/(a+b)$. For example, the hardness of titanium carbonitride, $TiN_{1-x}C_x$, which is miscible within the whole range of the C:N composition follows this rule: With *x* increasing from 0 to 1 the hardness monotonously increases from that of TiN to that of TiC (see Fig. 8 in Ref. 6 for plasma chemical vapor definition films with a low compressive stress of $<$0.5 GPa). A similar relationship applies for

a)Electronic mail: veprek@ch.tum.de

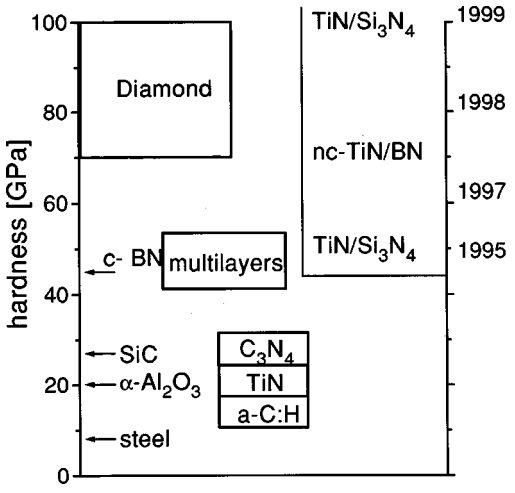


FIG. 1. Vickers hardness of selected materials in comparison with that of heterostructures and nanocrystalline composites (the numbers on the right-hand side indicate the year when the hardness given was achieved). Notice that the hardness of diamond depends on the quality and purity of the crystal and the ultrahard nanocomposites with $H_V \geq 100$ GPa have a substoichiometric $SiN_x$ (see the text).

the elastic modulus and fracture strength. For a given superlattice period or for a given fraction of the nanocrystalline and amorphous phases the superhardness reaches a maximum which exceeds that of the both phases by a factor of 3–5. Whereas much theoretical understanding of the mechanical properties of superlattices has been achieved during the last 20 years, there are many challenging questions remaining as to the understanding of the properties of superhard nanocomposites.

In this review we summarize the present status of the research and technological development in the field of superhard materials with emphasis on the nanostructured ones which are prepared as thin protective coatings. The reason is twofold: First, many papers and excellent reviews have been published recently on the preparation and properties of polycrystalline diamond and *c*-BN and, therefore, there is no need to repeat them. Second, in spite of the long term research and technological development in this field, practical applications of thin films made of polycrystalline diamond and *c*-BN are still rather limited. The reason is the high solubility of carbon in steel, silicon, and other alloys (carbide formation) in the case of polycrystalline diamond, and technological difficulties in deposition of sufficiently thick and adherent *c*-BN coatings, which so far has limited the applicability of this material to *c*-BN based ceramics.[1,2]

In Sec. II we shall discuss the meaning of hardness from both the theoretical and practical point of view. In Sec. III we briefly summarize intrinsic superhard materials. In Sec. IV the present status of the research and understanding of the nanostructured materials are described; Sec. IV is subdivided into Secs. IV A and IV B which are devoted to heterostructures and nanocomposites, respectively. In the latter, several questions that remain will be addressed and briefly discussed.

## II. MEANING AND MEASUREMENT OF HARDNESS

The hardness of a material is a measure of its ability to resist deformation upon a load.[7,8] The nature of that load defines various kinds of hardness. ''Theoretical'' hardness is the resistance of a material to deformation under isostatic pressure. It is proportional to the reciprocal value of the bulk modulus *B*. From Hooke's law $B = d\sigma/d\epsilon$(where $\sigma$ is the applied stress and $\epsilon$ the resulting elastic strain) and the relationship between the stress (a force) and the first derivative of the binding energy $E_b$ versus bond distance $a$ at the equilibrium position $a_0, \sigma = (dE_b/da)_0$, one obtains $B = (d^2E_b/da^2)_0$.[9] Thus, a high curvature of the interatomic potential curve at the equilibrium bond distance $a_0$, i.e., a high bond energy and small bond length result in a high theoretical hardness. A high bond energy means a high electron density between the atoms, as is found for a nonpolar, covalent bond between atoms of small radii of the first period. Obviously, a high coordination number is required in order to maximize the value of *B*. For these reasons carbon in its metastable, fourfold coordinated $sp^3$ hybridization, diamond polymorph, is the hardest material known, followed by cubic boron nitride, *c*-BN.[8]

Based on such general considerations and a semiempirical formula Sung and Sung predicted in 1984 that $C_3N_4$ should have a hardness comparable to that of diamond.[8] Later on, Cohen[10] and co-workers[11–13] derived formula (1) which reproduced very well the bulk moduli of many materials and confirmed the prediction of Sung and Sung regarding the theoretical hardness of $C_3N_4$.

$$B = \frac{\langle N_C \rangle}{4}(1971 - 220\lambda)a_0^{-3.5}. \quad (1)$$

Here, $\langle N_C \rangle$ is the average coordination number and $\lambda$ is the polarity of the bond; *B* is in GPa and $a_0$ is given in angströms.[12] For a nonpolar, covalent bond in diamond $\lambda = 0$ whereas in other compounds, such as *c*-BN, $Si_3N_4$, and $C_3N_4$, $\lambda > 0$. The expected high theoretical hardness of $C_3N_4$ is based on the small bond distance and the relatively small polarity $\lambda$ of the C–N bond.

As we shall see later, this prediction has not been confirmed by experiments thus far.[14–56] However, ''fullerene-like,'' cross-linked carbon nitride thin films $CN_x$ ($x \approx 0.25-0.35$) deposited by reactive dc magnetron sputtering at temperatures above 200 °C can reach a high hardness of 40–60 GPa.[57–61] This is an example of the well known rule that the microstructure determines the practically achievable strength (and hardness) of engineering materials which is orders of magnitude smaller than the theoretical strength $\sigma_c(\text{theor}) \cong G/2\pi$, where $\sigma_c$ (theor) is the theoretical critical fracture stress and *G* the shear modulus.[9,62–64] The reason for this is that the deformation and fracture of materials occur by the multiplication and movement of dislocations in crystalline materials and growth of microcracks in glasses and ceramics, all of which require a much smaller stress than the theoretical value $\sigma_c$ (theor) mentioned above.[9,62–64] Therefore, the practical strength and hardness of materials is de-

termined by the microstructure which hinders the multiplication and movement of dislocations and the growth of the microcracks.

Obviously, the theoretical hardness [Eq. (1)] is of little use in considering a material for an application. Instead, one has to consider the practically measured type of hardness depending on the particular applications. At least three categories of hardness have to be distinguished: scratch hardness (e.g., the Mohs scale used by mineralogists), static indentation hardness (e.g., Brinell, Vickers, or Knoop measurement), and rebound or dynamic hardness. In the last measurement the indenter is usually allowed to fall in the gravity from a given height which, together with the indenter mass, defines the impact energy.[7]

The static indentation measurements using the Vickers or Knoop technique are the only ones that can be relatively simply applied to the measurement of superhard materials. Therefore, they are being used for the characterization of materials by the majority of researchers. The Vickers indenter is a regular pyramid made of diamond with an angle of 136° between the opposite faces. The choice of this angle is based on an analogy with the Brinell test because both methods yield similar values of hardness[7] for relatively soft materials with $H \leqslant 1000$ kg/mm$^2$. During the measurement, the diamond pyramid is pressed into the material to be tested under a defined load $L$ (kg) and, after unloading, the average value of the two diagonals $d$ (mm) of the plastic deformation remaining is measured under a microscope. The Vickers hardness is proportional to the ratio of the applied load and the area of the plastic deformation $H = \text{const}\ L/d^2$ and given in units of kg/mm$^2$ or giga pascal (1000 kg/mm$^2$ = 9.807 GPa).[7,8] The Knoop hardness is measured in a similar way, but the diamond pyramid has two different angles, 172°30′ and 130°, thus yielding an elongated plastic deformation. The hardness is calculated from the longer diagonal whereas the shorter one yields information on the elastic properties.[7,8,65]

Modern indentometers for the measurement of the hardness of thin films use a computer controlled stepwise increase of the load up to a chosen maximum $L_{\max}$ followed by stepwise unloading.[66–71] Instead of measuring the diagonal of the plastic deformation, the indentation depth $h$ is measured electronically and the indentation curve evaluated (Fig. 2). The ''plastic hardness'' is calculated from the maximum load $L_{\max}$ and the depth of the plastic indentation $h_{\text{plastic}}$ as $H_{\text{plastic}} = L_{\max}/26.43(h_{\text{plastic}})^2$. The ''universal hardness'' $H_u$ is obtained from the same formula if $h_{\max}$ is used instead of $h_{\text{plastic}}$. The universal hardness includes both elastic and plastic deformation. The linear part of the unloading curve corresponds to the elastic recovery when the diamond pyramid is in constant area contact with the material. Therefore it represents Hooke's law and allows one to calculate the corresponding ''elastic modulus'' $E/(1-\nu^2)$, $\nu$ being the Poisson ratio. For superhard materials, the elastic deformation of the diamond has to be accounted for and the measured $E/(1-\nu^2)$ value corrected.[69,70] Details of the apparatus, the measuring procedure, and possible errors are given in Refs.

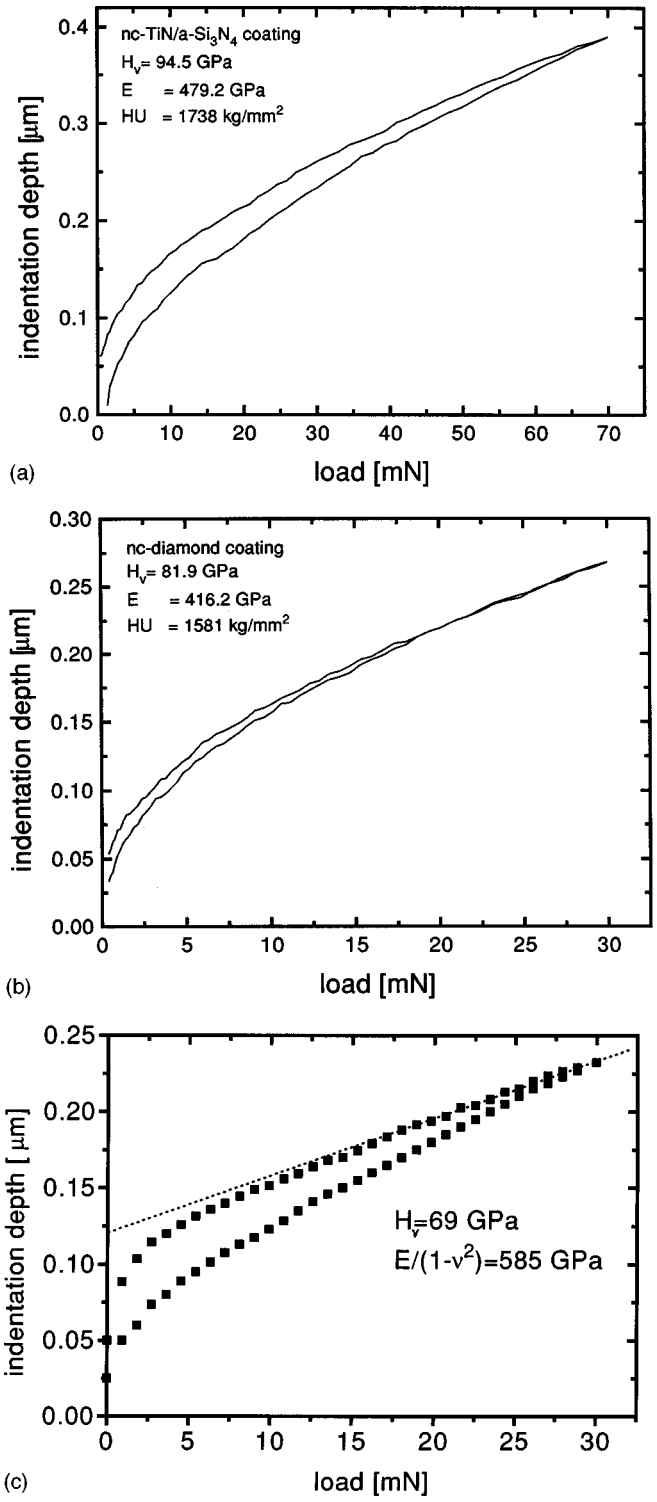


FIG. 2. (a) Example of the indentation curve measured on a 3.5 $\mu$m thick layer of *nc*-TiN/SiN$_x$. The lower curve is the loading, and the upper one the unloading part. (b) Indentation curve measured on a 1.5 $\mu$m thick single phase nanocrystalline diamond coating. (c) Indentation curve measured on about 3 $\mu$m *nc*-TiN/BN coatings deposited on WC–Co cemented carbide (''hard metal'') by a combined plasma PVD and CVD technique. $H_V$ means the plastic Vickers hardness, *HU* the universal hardness, and *E* the elastic modulus corrected for deformation of the diamond. Notice that the *nc*-TiN/SiN$_x$ coating was measured at a higher maximum load of 70 mN where the measured hardness of the *nc*-diamond has already decreased (see Fig. 4).

66–71. If done correctly, the plastic hardness measured by the indentation agrees within about 10%–20%, reasonably well with that from the classical Vickers method in the range of $H \leqslant 12$ GPa.[67] However, for superhard films deposited on a tough substrate we have found that the value determined from the indentation curve is typically about 30%–40% smaller than that determined by the classical Vickers technique from the diagonal of the remaining plastic indentation. For example, for a 4 $\mu$m thick $nc$-TiN/$a$-$Si_3N_4$ coating on a stainless steel substrate the indentation yields a load independent ''plastic'' hardness of 45 GPa (the maximal load is 35–70 mN) whereas the classical Vickers technique yields 60–80 GPa.[72] This reflects a fundamental problem associated with the hardness measurement of superhard coatings: In order to exclude the effects of the deformation of the substrate, the indentation depth should not exceed 5% of the film thickness. [Various papers report a higher value (e.g., up to 10%),[67] but our experience has shown that in the case of superhard coatings 5% of the coating thickness is a safer upper limit. Of course, this rule of thumb is only a rough guideline for measurements on superhard coatings and it should be carefully checked in any particular measurement.] This means that, even with relatively thick coatings of 5 $\mu$m, the maximum indentation thickness is limited to less than about 250 nm. Therefore the value of the hardness measured by the automated indentation technique may be subjected to a number of possible errors unless many corrections are carefully done and the whole indentation curve is carefully evaluated.[67,69,71]

Many possible errors are even more likely to occur by the so called ''nanoindentation'' technique which is frequently used to measure very thin films and the indentation depth is in the range of $\leqslant$10–20 nm.[69–71] For example, when measuring soft materials, such as aluminum or pure iron with a small load and indentation depth, the dislocations are pinned in the surface contaminant layer (oxides, carbides) and, consequently, unrealistically high values of hardness are found. The plastic deformation may also need a certain time to reach equilibrium under the given load because of a finite velocity of dislocation movement and crack growth. This can be seen as creep (an increase of the indentation depth) when a constant load is applied for a period of $\geqslant$60 s. An indentation depth of 20 nm is comparable with the flattened part of the indenter tip which has a typical radius of 200 nm and emphasizes the need for a careful correction.[67] Last but not least, an indentation depth of the order of 20–100 nm is comparable to the surface roughness of the majority of the coatings which again falsifies the measured data.[67,72,73] Therefore, such measurements have to be carefully checked for all the possible errors that have been discussed in the literature.[66,67,69–71]

In order to obtain reliable results of the hardness of superhard materials, one should always used at least $\geqslant 5$ $\mu$m thick films with small surface roughness, make sure that the maximum indentation depth $h_{max}$ does not exceed 5%–10% of the film thickness, check for possible dynamical response of the material by sustaining the indenter at the maximum load $L_{max}$ for at least 60 s, and measure the hardness (always at a different position on the layer) as a function of the maximum applied load. (Repetitive indentations at the same place may provide interesting information on the material's properties. However, in many cases it can result in ''work hardening'' which falsifies the real value of the hardness of the material. For example, we have found that superhard $nc$-TiN/$a$-$Si_3N_4$ nanocomposites with a carefully measured hardness of about 50 GPa show, after several repetitive indentations at the same place, an ''apparent hardness'' of $\geqslant$150 GPa.) Only load independent values of the hardness which do not show any creep can be considered as reliable. An example of such measurements and evaluation can be found in Fig. 2 of Ref. 74. Unfortunately, many papers do not follow this measuring procedure and, therefore, the reported values of the superhardness may be subjected to errors.

Furthermore, compressive stress which is frequently found in coatings deposited by plasma induced chemical vapor deposition (CVD) or physical vapor deposition (PVD), such as sputtering or vacuum arc evaporation under high energy ion bombardment, increases the apparent hardness by a value which may be significantly larger than that corresponding to the stress. Thus, too high values of the hardness by much more than 10 GPa can be incorrectly measured and reported (see Sec. III C).

Even if one takes into account all these problems one should keep in mind that the Vickers technique, which was originally developed for conventional alloys and materials with hardnesses $\leqslant$20 GPa, is up to its limit when measuring materials whose hardness approaches that of diamond. Thus, the values of hardness of 70–80 GPa which are often found using the above described careful procedure in nanocrystalline composites[6,75–77] should be taken as a relative measure of the hardness only. For a critical review of the indentation technique see Refs. 67 and 69–71.

As already emphasized, hardness is only one of many properties which are important for applications.[1,2,78] The Vickers indentation technique enables one in principle to also determine the fracture toughness of a material from the critical load which is needed to initiate radial cracks which typically propagate from the corners of the indentation.[71,79–81] However, experience with superhard nanocomposites has shown that, because of their high elasticity and high toughness, only circular cracks within the crater but no radial ones are formed even if the indentation depth is larger than the thickness of the coatings so that the indenter penetrates into the substrate.[72] Indentation into 10.7 $\mu$m thick $nc$-TiN/$a$-$Si_3N_4$ nanocomposites with a load of 1000 mN resulted in no crack formation thus indicating the high toughness of such coatings.[82]

These problems with measurements of superhard coatings may possibly be resolved by using the concept of hardness as the increase of energy density upon deformation.[8,58,69] This applies to both the theoretical as well as the practical hardness. The latter has recently been elaborated on by Rother

and co-worker.[83–86] The basis of this approach is the relationship,

$$W_i = e_V \cdot h^3 + e_A \cdot h^2, \quad (2)$$

where $W_i$ is the total deformation energy produced by the indenter in the material under testing, $e_V$ and $e_A$ are the specific energy densities due to densification and shear displacement, respectively, and $h$ is the indentation depth. The slope of the plot of the second derivative of $W_i$, i.e., of the first derivative of the applied load, versus the indentation depth yields the specific energy $e_V$. The results published so far suggest that this meaning of hardness may be more universal than that of Vickers or Knoop.[86] Preliminary study supports this approach as also being more appropriate for superhard materials.[72] In a similar way, the area of the indentation curve (see Fig. 2) can be used to calculated the total work of the indentation[69] and its elastic and plastic components.[58]

## III. INTRINSICALLY SUPERHARD MATERIALS

### A. Diamond and cubic boron nitride

There are only two confirmed phases of intrinsic superhard materials, diamond and *c*-BN. Diamond, a metastable, high pressure, high temperature modification of carbon[87,88] with a hardness ranging between about 70 and 100 GPa (90 GPa is a more realistic value[8]), is the hardest material because of its fourfold covalent bond and small atomic size which result in a strong, short, nonpolar bond. The hardness depends on the quality of the crystals (see, for example, Ref. 89, and references therein). Depending on the content of nitrogen and other impurities (originally, the color and transparency were the basis for this categorization) as well as on dislocations, several types of natural diamonds are distinguished; here only the most important are mentioned: type Ia diamond contains up to 0.1 at. % nitrogen incorporated as pairs of N atoms, whereas in the type Ib isolated N atoms are present. Type II diamonds have virtually no nitrogen and type IIa is colorless, whereas type IIb is blue due to incorporated boron. (With increasing analytical sensitivity the number of such diamonds shrinks.) Crystals with nitrogen doping of about $3\times10^{19}$ N atoms/cm$^3$(about 0.02 at. %) have the highest hardness which decreases for both, a higher and a lower nitrogen content.[90]

Cubic boron nitride, *c*-BN, is the second strongest and hardest material ($H\approx48$ GPa). In 1961 Wentorf determined the equilibrium diagram showing that *c*-BN is a metastable, high pressure, high temperature phase.[91] His data were confirmed and improved upon in several later papers.[87,92] Recent calculations suggest that *c*-BN may be the stable modification under standard conditions (1 bar, 298 K, see Ref. 93, and references therein). Whereas diamond occurs in nature, only synthetic *c*-BN is known. Both diamond and *c*-BN are industrially prepared by high pressure of $\geqslant5$ GPa and temperature $\geqslant1600$ °C metal-catalyzed solution growth techniques. Diamond growth utilizes a higher solubility of graphite in metals, such as Fe, Ni, and others, compared to diamond. Cubic *c*-BN is grown from a melt of quasibinary nitrides like, e.g., $Li_3BN$.[87] Worldwide production of diamond and *c*-BN amounts to several hundred tons.[87,88]

For conventional cutting tools, small diamond crystallites prepared by high-pressure and -temperature synthesis are imbedded into an appropriate metal. The high solubility of carbon in iron and in many other metals limits the application of diamond tools to aluminum alloys, ceramics, glasses, wood, etc. Compared to diamond, *c*-BN does not dissolve in most metals and is stable to oxidation in air to high temperatures of $>1000$ °C. Therefore, ceramics fabricated from *c*-BN crystallites by hot sintering with appropriate binders are used for a wide range of cutting tools because of their hardness and thermal stability which are superior to conventional WC–Co ''hard metal.''[1,2]

Diamond and *c*-BN can be also prepared by CVD, at relatively low pressure and temperature, using kinetically controlled growth in the metastable region.[94] As early as 1959 Eversole filed a patent for low pressure growth of diamond by CVD from hydrocarbons and from a mixture of $CO/CO_2$.[95] This technique was further developed by Angus and co-workers[96–98] and by Deryagin *et al.*[99–101] Schmellenmeier was probably the first researcher who reported on low pressure, glow discharge plasma induced deposition of carbon films that contained diamond crystallites.[102,103] Aeisenberg and Chabot,[104,105] Spencer *et al.*,[106] and Strelnitskii *et al.*[107] deposited polycrystalline diamond films from an ion beam containing $Ar^+$ and $C^+$ ions. Later on several CVD techniques including hot wire, microwave discharge, plasma jets, and flames were developed which allow one to deposit polycrystalline diamond films at atmospheric or low pressure at temperatures between about 600 and 1000 °C.

These techniques are based on kinetically controlled preferential nucleation and growth of diamond crystallites and faster etching of the simultaneously formed graphite nuclei. In order to facilitate such conditions the deposition is performed close to the solubility of carbon in the gas phase which contains typically hydrogen and/or oxygen. This is summarized in a C–H–O diagram by Bachmann *et al.*[108] Nanocrystalline, single phase diamond films were also deposited from various gas mixtures including a hydrogen-free mixture of argon and fullerenes.[109] Compared to the coarse grained polycrystalline films that are typically obtained from C–H–O gas mixtures *nc*-diamond films offer many advantages. The high thermal-expansion mismatch between the diamond and the WC–Co hard metal substrate, the low nucleation density of diamond on WC–Co, and the high solubility of carbon in cobalt prevented the coating of WC–Co cemented carbide cutting tools. This adhesion issue has recently been solved by the application of appropriate interlayers and several companies are now selling cutting tools coated with CVD polycrystalline diamond.[94] For further details on the development and applications of polycrystalline CVD diamond films we refer the reader to the recent reviews.[110,111]

Much research effort has been devoted to plasma CVD of *c*-BN films (e.g., see Refs. 36 and 112, and references

therein). In a way similar to the deposition of amorphous hard carbon (see below), the formation of the fourfold coordinated network of the *c*-BN phase requires energetic ion bombardment. Both plasma PVD and CVD were used in a large number of studies. However, BN films with a high fraction of the cubic phase have high compressive stress of several GPa (Ref. 112) or even up to 25 GPa (Ref. 113) as a result of energetic ion bombardment. This causes severe peeling of when the film thickness exceeds about 300 nm. Work on the preparation and properties of *c*-BN by plasma activated deposition techniques was summarized in several recent papers[114] and reviews[36,112] to which we refer the reader.

Worth mentioning also is hard amorphous carbon *a*-C:H [sometimes called ''diamond like'' hard carbon (DLHC)] which is obtained by plasma induced CVD from hydrocarbons at a low pressure of typically $\leqslant 0.5$ mbar and bombardment with energetic ions of about 100 eV. The first report on its preparation was by Holland and Ojha[115–117] and was followed by extensive research in many laboratories (see e.g., Refs. 118–127). Ion bombardment promotes the formation of fourfold coordinated carbon because of the difference of the displacement energy for the graphitic $sp^2$ (about 20 eV) and the diamondlike $sp^3$ (50–80 eV) C atoms.[126,127] Although the hardness of this material reaches only about 20 GPa, its very low coefficient of friction of $\leqslant 0.1$ (Ref. 121) makes it interesting for many applications including lubricant-free bearings, magnetic storage hard disk, various cutting tools, and machine parts (see, Refs. 128 and 129, and references therein).

### B. $C_3N_4$ and $CN_x$

Like diamond and *c*-BN, $C_3N_4$ is a thermodynamically unstable compound whose preparation requires rather extreme conditions. In the case of plasma CVD several conditions have to be met simultaneously:[14]

(1) a high degree of dissociation of nitrogen which provides a high flux of low energy atomic nitrogen of the order of $10^{19}-10^{20}$ N atoms/cm$^2$ s towards the surface of the growing film in order to achieve the desired stoichiometry;
(2) a medium energy ion bombardment to promote the carbon into the metastable fourfold coordination; and
(3) a relatively high temperature of about $\geqslant 800$ °C in order to evaporate the paracyanogen$(CN)_n$, which is always formed during the deposition of stoichiometric $C_3N_4$ (see Ref. 14 for further details).

However, the Vickers hardness reported for stoichiometric amorphous $C_3N_4$ films reached only about 30 GPa, which is much less than that of diamond and many other superhard materials. Using similar synthetic principles, other authors succeeded in the deposition of crystalline, stoichiometric $C_3N_4$ films[15–20] but they could not measure the hardness because of the insufficient density of the polycrystalline films.[16]

A large number of papers have reported on the ''synthesis of carbon nitride'' but these ''carbon nitride'' films are highly substoichiometric, having a large nitrogen deficiency even below that of paracyanogen and a lower hardness.[21–48] [Paracyanogen is a $(CN)_n$ polymer consisting of six-member –C–N–C–N–C–N– rings with alternating double bonds, the fourth valence of carbon being used for the bond to the neighboring ring.[88] It can be prepared by polymerization of dicyanogen $(CN)_2$ or by plasma CVD (see Refs. 14 and 88, and references therein).] The reason for the failure to approach the stoichiometry of $C_3N_4$ is the obvious neglect of the above mentioned simple principles for its synthesis by means of activated deposition.[14] Indeed, all the techniques which were used in these papers were lacking either a sufficiently high flux of low energetic atomic nitrogen towards the surface during deposition, or a high temperature or suitable medium energy ion bombardment. Computer simulation and measurements clearly show that energetic ion bombardment, which is needed to promote the carbon into the metastable fourfold coordination ($sp^3$ hybrid), also leads to a loss of nitrogen from the film,[48,49] thus making the synthesis of the stoichiometric $C_3N_4$ by means of techniques such as sputtering, energetic ion beam deposition, arc evaporation, etc.[21–48] unlikely.

This has been summarized in several papers and we refer the reader to Refs. 49–55 for further details. Of particular interest are the critical papers by De Vries[50] and the excellent critical review by Korsounskii and Pepekin[53] which also contains a suggested phase diagram of the expected stability of $C_3N_4$ at high pressures and temperatures.

Efforts to prepare $C_3N_4$ by exposing carbon and nitrogen containing organocompounds to high pressure have resulted so far in the formation of diamond and nitrogen. The reason for this is most probably the high thermodynamic instability of $C_3N_4$,[14] with an estimated Gibbs free energy of formation of $\Delta G_f^0 = 170-227$ kJ/mole.[53] Accordingly, $C_3N_4$ should be stable only at a pressure that is higher than that of the graphite-to-diamond transformation, e.g., $\geqslant 40-60$ GPa for temperatures of 2000–3000 K, respectively (see Fig. 2 in Ref. 53). Therefore, a carbon and nitrogen containing compound, when exposed to high pressure, will decompose into diamond and $N_2$ unless the activity and activation energy of nitrogen are sufficiently increased, e.g., by an appropriate metallic solvent. The recent publication by He *et al.*[54] reports on a successful preparation of microcrystalline $\alpha$- and $\beta$-$C_3N_4$ at a high pressure of 7 GPa and temperature of 1400 °C with nickel-based alloy and cobalt as catalysts. This paper by He *et al.* does not report on the mechanical properties of the material.

One remark should be made regarding a number of papers that reported on the preparation of $CN_x$ with a ''high nitrogen content'' from various nitrogen-rich organo- or azidocompounds (see, e.g., Ref. 130). The materials obtained may have had a relatively high content of nitrogen, but these materials were of a polymeric nature and had nothing in common with ''superhard'' $C_3N_4$. This is easily seen by compar-

ing the reported infrared spectra of these products with that reported[14,32] and predicted[56] for $C_3N_4$.

Substoichiometric $CN_x$ thin films may nevertheless find some applications such as protective, low friction coatings, e.g., on magnetic storage disks[21–25] or as field emission tips.[47] In order to provide high memory density the thickness of the overcoat on the magnetic disks must be in the range of 10 nm. The hardness of $CN_x$ films with nitrogen contents of 10–30 at. % is less than 30 GPa. This is, however, higher than the hardness of hydrogenated hard carbon (*a*-C:H, typical $H_V \simeq 7-15$ GPa) which is used presently for magnetic disk overcoats. Beside the higher hardness, the overcoats have to also have good sliding resistance, low wear, and chemical stability. $CN_x$ overcoats have shown superior properties compared to these of *a*-C:H.[21–23]

However, these films are not superhard. In order to reach a superhardness of 40–50 GPa the deposition of the $CN_x$ films has to occur at elevated temperature.[57–61] The properties of these films prepared by magnetron sputtering in nitrogen are a complex function of deposition temperature, nitrogen pressure, and the concomitant compressive stress. Films grown at 350 °C show the highest hardness and elasticity.[60,61] This materials, also called ''fullerenelike,'' resemble a disordered, cross-linked graphite-like structure with odd-membered rings in which the relative low concentration of nitrogen, $CN_{0.25-0.35}$, causes undulation of the graphitic basal planes. The high hardness combined with high elasticity and self-lubricant properties may open up interesting applications.

### C. Miscellaneous superhard materials

We shall now summarize various other intrinsic superhard materials. The B–C–N system is rich in hard and superhard materials, the majority of them being refractory ceramics. Boron carbon nitrides can form a relatively soft graphite-like (''hexagonal'') phase or a superhard cubic or amorphous phase. The first report of the deposition of the ternary $BC_xN_y$ films by thermal CVD was by Badzian *et al.*[131] who also used microwave plasma for this process and obtained deposits with a cubic modification as was seen by x-ray diffraction (XRD).[132] The plasma activated CVD was also used later on by Montasser *et al.*,[133,134] Levy *et al.*,[135] and by Besmann[136] who achieved a hardness between 4 and 33 GPa depending on the deposition conditions. Further work has shown that, similar to the deposition of hard *a*-C:H diamond-like hard carbon (DLHC) and *c*-BN, the high hardness of the $BC_xN_y$ films requires an appropriate ion bombardment and an elevated deposition temperature.[137] More recently Riedel and co-workers[138–140] prepared superhard $BC_4N$ coatings by plasma CVD from single source organometallic precursors, pyridine borane ($C_5H_5NBH_3$) and triazaborabicyclodecane $[BN_3H_2(CH_2)_6]$. The coatings were amorphous and the hardness showed a large variation depending on the deposition conditions which have not been adequately characterized so far. The highest hardness of 64 GPa, which was reported by these researchers, clearly shows that the C–B–N triangle is worth being elucidated in more detail. Superhardness of $\geqslant$60 GPa was also reported for *c*-BN doped with about 7 mol % of $B_4C$,[141] or with about 3.5 wt % of C (Ref. 142) at high temperatures of 1900–2000 °C and pressure of 5 GPa. The relatively soft hexagonal boron carbon nitride prepared by CVD[131] could be transformed into a hard cubic polymorph by a high temperature (3000 °C) and pressure (14 GPa) treatment.[132] Also, incorporation of silicon into the boron carbon nitride resulted in promising materials.[140] However, more research is needed.

In that context it is also worth mentioning the high hardness of amorphous *a*-$B_4C$ of $\geqslant$50 GPa which was prepared by very high frequency plasma CVD[143,144] with a negligibly low stress or by reactive magnetron sputtering.[145] Although in the latter case the compressive stress of $\leqslant$6.7 GPa may have enhanced the measured apparent hardness of $\leqslant$72 GPa, these amorphous films were in the range of superhardness. On the other hand, crystalline $B_4C$ shows a lower hardness of about $\leqslant$30 GPa.[146] Stoichiometric single crystalline boron carbide has the exact stoichiometry of $B_{13}C_3$. It consists of boron icosahedra which are connected by carbon and boron atoms.[88,147] Therefore, amorphous $B_4C$ may be regarded as a composite consisting of the icosahedral boron quasicrystals imbedded in an amorphous matrix. There appears to be a certain similarity in the hardness and strength enhancement observed in nanocrystalline/amorphous composites (see below) as well as in aluminum alloys $Al_{96-x}Cr_3Ce_1Co_x$ ($x = 1\%-2\%$) consisting also of quasicrystals, where very high enhancement of the strength by a factor of 7 was found.[148] Although boron carbide suffers from relatively low oxidation resistance in air due to fast oxidation at $\geqslant$450 °C, the occurrence of the superhardness is challenging.

The great potential of the B–C–N triangle can be extended further when ternary and quanternary compounds with silicon are included. For example, $\alpha$-SiC has a hardness of about 26 GPa,[146] but it can be increased up to 40 GPa by an admixture of small amounts of boron to form strong grain boundaries in hot-pressed SiC ceramics.[149] Badzian *et al.* reported high hardness of about 63 GPa for crystalline $B_{12}C_{2.88}Si_{0.35}$ and 65 GPa for $Si_3N_{2.2}C_{2.16}$.[150] Silicon carbon nitride appears to be a very promising material.

Knotek and co-workers reported on superhard Ti–B–C–N coatings deposited by magnetron sputtering[151,152] in which a maximum hardness of about 55 GPa was found. Also, $TiB_2$ coatings prepared by magnetron sputtering were reported to have a hardness of up to 70 GPa,[151,152] and similar superhardness was reported for other plasma PVD systems (e.g., Ti–B–N and Ti–B–C,[151,152] and in some other papers that will be discussed in Sec. IV B).

However, it is not quite certain whether such high values of hardness reported for plasma PVD coatings are indeed intrinsic properties of these materials. As already mentioned in Sec. II A, plasma CVD[153] and PVD[154] films deposited under high energy ion bombardment have, typically, a high compressive stress of 5–10 GPa which can be annealed out at 600–700 °C. These films show a high hardness which, upon annealing, decrease much faster than the stress. Herr and Broszeit[155] reported recently, for example, a decrease of

the apparent hardness of TiN films from 36 to 27 GPa when the compressive stress decreased from 6.7 to 2.1 GPa upon annealing at 650 °C. Similar results were found for all films studied in that work. In the case of $HfB_2$ deposited at the lowest pressure of 0.5 Pa (which yields the highest compressive stress in the coatings), the apparent hardness decreased from about 72 to about 17 GPa upon such an annealing. These examples give us a warning that extreme care has to be exercised when measuring and reporting such high hardness values.

Badzian *et al.* reported on superhard boron suboxide $B_{22}O$ which ''easily wore the (001) surface of diamond and scratched the (111) face.''[156] The material was prepared by solid-state reaction from a stoichiometric mixture of boron and $B_2O_3$ at 1600–2000 °C.[157] The reported hardness was about 60 GPa. Thus, the wear of the (001) and scratching of the (111) faces of diamond were due to a different crystallographically anisotropic wear mechanism rather than due to higher hardness. These surprising properties of $B_{22}O$ were attributed to the presence of interstitial oxygen within the boron lattice.[156] These researchers also reported on the deposition of boron suboxide films with oxygen contents of 5–30 at. % by magnetron sputtering, but no hardness was measured. More recently Tsui *et al.*[158] prepared boron suboxide in a similar way with about 11 at. % oxygen and measured a hardness of only $\leqslant$28 GPa. Thus, this material remains a challenge for further research.

Sapphire, with about 21 GPa, is the hardest stable oxide.[159] Recently Léger *et al.*[160] reported on the high pressure synthesis of stishovite (a high pressure modification of silica), with the highest hardness of 33 GPa found for stoichiometric oxide materials so far. Since high pressure modifications have higher density, one may ask if there is a possibility of obtaining even harder oxides. Because sufficiently large crystals (which one needs for the hardness measurements) are rarely available, one can estimate if a material may become superhard by a comparing its bulk moduli. (The bulk modulus of small crystals can be measured, e.g., from the pressure dependence of the lattice constant by XRD in a high pressure cell.) The hardness of bulk moduli of various materials show a fairly good correlation.[161] A high value of 399 GPa was reported for the high pressure (pressure $\geqslant$12 GPa) cubic modification of $RuO_2$.[161,162] Lundin *et al.* have calculated the bulk moduli of several high pressure modifications and obtained high values, thus suggesting that these phases may also be superhard. In particular, they obtained for the high pressure modification of $RuO_2$ a value of 434 GPa, in a reasonable agreement with the experimentally reported one, and 411 GPa for a high pressure modification of $OsO_2$.[163]

## IV. NANOSTRUCTURED SUPERHARD MATERIALS

As mentioned in Sec. II, the strength and hardness of engineering materials are orders of magnitude smaller than the theoretical one. They are determined mainly by the microstructure which has to be designed in such a way as to efficiently hinder the multiplication and movement of dislocations and the growth of microcracks. This can be achieved in various ways known from metallurgy, such as the solution, work, and grain boundary hardening (see, e.g., Refs. 9, 64, and 148). In this way, the strength and hardness of a material can be increased by a factor of 3–7, i.e., superhard material should form when such enhancement can be achieved starting from a hard material ($H_V \geqslant 20$ GPa).

The solution and work hardening do not operate in small nanocrystals about $\leqslant$10 nm because solute atoms segregate to the grain boundary and there are no dislocations. Therefore we consider the possibilities of extending the grain boundary hardening in poly- and microcrystalline materials, described by the Hall–Petch relationship,[9,164,165] Eq. (3), down to the range of a few nanometers.

$$\sigma_C = \sigma_0 + \frac{k_{\mathrm{gb}}}{\sqrt{d}}. \tag{3}$$

Here $\sigma_C$ is the critical fracture stress, $d$ the crystallite size, and $\sigma_0$ and $k_{\mathrm{gb}}$ are constants. Many different mechanisms and theories describe Hall–Petch strengthening:[9,64,164–166] Dislocations pileup models and work hardening yield the $d^{-1/2}$ dependence but different formulas for $\sigma_0$ and $k_{\mathrm{gb}}$ whereas the grain–grain boundary composite models also give a more complicated dependence of $\sigma_C$ on $d$.

The strength of brittle materials, such as glasses and ceramics, is determined by their ability to withstand the growth of microcracks. [Brittle materials do not undergo any plastic deformation up to their fracture. Their strength (and hardness) is proportional to the elastic modulus.[9] Superhard nanocrystalline composites (see Sec. IV B) show such behavior, but they have also a very high toughness.] The critical stress which causes the growth of a microcrack of size $a_0$ is given by a general formula,

$$\sigma_C = k_{\mathrm{crack}} \sqrt{\frac{2E\gamma_s}{\pi a_0}} \propto \frac{1}{\sqrt{d}}. \tag{4}$$

Here $E$ is the Young's modulus, $\gamma_s$ the surface cohesive energy, and $k_{\mathrm{crack}}$ is a constant which depends on the nature and shape of the microcrack and on the kind of stress applied.[9] Thus, the $d^{-1/2}$ dependence of the strength and hardness in a material can also originate from the fact that the size $a_0$ of the possible flaws, such as voids and microcracks which are formed during the processing of the material, also decreases with decreasing grain size. For these reasons, the Hall–Petch relationship, Eq. (3), should be considered as a semiempirical formula which is valid down to a crystallite size of 20–50 nm (some models predict an even higher limit[166,167]).

With the crystallite size decreasing below this limit, the fraction of the material in the grain boundaries strongly increases which leads to a decrease of its strength and hardness due to an increase of grain boundary sliding.[167–176] A simple phenomenological model describes the softening in terms of an increasing volume fraction of the grain boundary material $f_{\mathrm{gb}}$ with the crystallite size decreasing below 10–6 nm:[177]

$$H(f_{\mathrm{gb}}) = (1 - f_{\mathrm{gb}})H_c + f_{\mathrm{gb}}H_{\mathrm{gb}}, \tag{5}$$

with $f_{gb} \propto (1/d)$. Due to the flaws present, the hardness of the grain boundary material $H_{gb}$ is smaller than that of the crystallites $H_c$. Thus the average (measured) hardness of the material decreases with $d$ decreasing below 10 nm. The first report of reverse (or negative) Hall–Petch dependence was by Chokshi *et al.*[178] Later on it was the subject of many studies, with controversial conclusions regarding the critical grain size where ''normal'' Hall–Petch dependence changes to the reverse one.[172,173,179–186] Sanders *et al.*[187–190] have recently shown that if nanocrystalline Cu and Pd samples prepared by inert gas condensation were compacted at elevated temperature, this critical grain size decreased to almost 10 nm. The improvement of the compaction was documented by small angle neutron diffraction.[190] Musil and Regent[191] reported softening of dense nanocrystalline NiCr thin films prepared by argon ion sputtering to occur below 7 nm.

Various mechanisms of grain boundary creep and sliding were discussed and are described by deformation mechanism maps in terms of the temperature and stress.[9,192–198] Theories of grain boundary sliding were critically reviewed in Ref. 166. Recent computer simulation studies[176] confirm that the negative Hall–Petch dependence in nanocrystalline metals is due to the grain boundary sliding that occurs due to a large number of small sliding events of atomic plains at the grain boundaries without thermal activation and, therefore ''will ultimately impose a limit on how strong nanocrystalline metals may become.''[176] Although many details are still not understood, there is little doubt that grain boundary sliding is the reason for softening in this crystallite size range. Therefore, a further increase of the strength and hardness with decreasing crystallite size can be achieved only if grain boundary sliding can be blocked by appropriate design of the material. This is the basis of the concept for the design of superhard nanocomposites which will be discussed in Sec. IV B.

As mentioned in Sec. I, another possible way to strengthen a material is based on the formation of multilayers consisting of two different materials with large differences in elastic moduli, sharp interface, and small thickness (lattice period) of about 10 nm.[5] Because this design of nanostructured superhard materials was suggested and experimentally confirmed before superhard nanocomposites were developed, we will deal with heterostructures in Sec. IV A.

### A. Heterostructures

In a theoretical paper published in 1970[5] Koehler suggested a concept for the design of strong solids which are nowadays called heterostructures or superlattices. Originally he suggested depositing epitaxial multilayers of two different metals, M(1) and M(2), having as different elastic constants as possible $E_{M(2)} > E_{M(1)}$ but a similar thermal expansion and strong bonds. The thickness of the layers should be so small that no dislocation source could operate within the layers. If under applied stress a dislocation, which would form in the softer layer M(1), would move towards the M(1)/M(2) interface, elastic strain induced in the second layer M(2) with the higher elastic modulus would cause a repulsing force that would hinder the dislocation from crossing that interface. Thus, the strength of such multilayers would be much larger than that expected from the rule of mixture (which was defined in Sec. I).

Koehler's prediction was further developed and experimentally confirmed by Lehoczky who deposited Al–Cu and Al–Ag heterostructures and measured their mechanical properties.[199,200] According to the rule of mixture, the applied stress $\sigma_a$ which causes elastic strain $\epsilon$ is distributed between the layers in proportional to their volume fractions $V_{M(x)}$ and elastic moduli $E_{M(x)}$. Lehoczky has shown that the tensile stress–strain characteristics measured on multilayers consisting of two different metals displayed a much higher Young's modulus and tensile strength, both of which increased with decreasing thickness of the double layer (layer period). For layer thicknesses of $\leqslant 70$ nm the yield stress of Al/Cu multilayers was 4.2 times larger and the tensile fracture stress was 2.4–3.4 times larger than the values given by the rule of mixture.

This work was followed by work of a number of researchers who confirmed the experimental results on various metallic multilayer systems [e.g., Cu/Ni, (Refs. 201–203)] as well as on superhard epitaxial and polycrystalline superlattices of nitrides such as TiN/VN,[204] TiN/NbN,[205–207] $TiN/V_xNb_{1-x}N$,[208–211] Ti/TiN, Hf/HfN, and W/WN,[212] oxides,[213–215] and superlattices consisting of transition metal nitride and $CN_x$.[216–221] In all these cases, an increase of the hardness by a factor of 2–4 was achieved when the lattice period decreased to about 5–7 nm. In the case of heterostructures prepared from materials with a hardness of $\geqslant 20$ GPa, such as transition metal nitrides, an increase by a factor of 2 is sufficient to reach superhardness of $\geqslant 40$ GPa. The maximum hardness reported for TiN/NbN superlattice with a lattice period of 4 nm was 50 GPa,[205] for TiN/VN it was about 55 GPa.[204] This work on heterostructures was summarized in excellent reviews[222,223] to which we refer the reader and also included early theories.

For a large lattice period, where the dislocation multiplication source can still operate, the increase of the hardness and the tensile strength (most researchers measured the hardness because it is simpler than the measurement of tensile strength done by Lehoczky[199,200]) with decreasing layer thickness is due to the increase of the critical stress needed to multiplicate dislocations $\sigma_c = Gb/l_{pp}$ ($G$ is the shear modulus, $b$ the Burgers vector, and $l_{pp}$ is the distance between the dislocation pinning sites[9]). Usually one finds strengthening dependence similar to the Hall–Petch relationship but with a somewhat different dependence on the layer period $\lambda^{-n}$ [instead of the crystallite size $d$ in Eq. (3)] with $n = 1/2$ for layers with different slip systems and $n = 1$ for layers with a similar slip systems.[222] More recent theoretical discussion of the Hall–Petch relationship for superlattices was published by Anderson and Li.[223] According to their calculations, strong deviations from continuum Hall–Petch behavior occurs when the thickness of the layers is so small that the pileup contains only one to two dislocations.

In brief: In thin layers where no dislocation source can operate and the Koehler and Lehoczky model applies, the

maximum value of the critical shear stress $\sigma_c(\lambda)$ which can cause movement of a dislocation from weaker layer 1 into stronger layer 2 is given by[5,199,200]

$$\sigma_c(\lambda) = \frac{G_{M(2)} - G_{M(1)}}{G_{M(2)} + G_{M(1)}} \frac{G_{M(1)}(\lambda_1 - 4b)\sin\varphi}{8\pi(\lambda_1 - 2b)}. \quad (6)$$

Here $G_{M(x)}$ are the shear moduli of the two materials, $\lambda_1$ is the thickness of the softer layer, $b$ is the Burgers vector of the dislocation, and $\varphi$ is the angle between the dislocation slip plane in layer M(1) and the interface M(1)/M(2). This theory predicts that the strength (and hardness) depends mainly on the relative difference between the shear moduli $(G_{M(2)} - G_{M(1)})/(G_{M(2)} + G_{M(1)})$ and the angle $\varphi$. For a small period but still $\lambda_1 \geqslant 4b$ the enhancement reaches an asymptotic value of

$$\sigma_c(\max) = \frac{G_{M(2)} - G_{M(1)}}{G_{M(2)} + G_{M(1)}} \frac{G_{M(1)}\sin\varphi}{8\pi}, \quad (7)$$

as experimentally confirmed by Lehoczky for Al–Cu and Al–Ag heterostructures.[199,200] However, in superhard heterostructures consisting of transition metal nitrides and Cu–Ni a decrease of the hardness was found when the lattice period $\lambda$ decreased below about 5–7 nm.

The decrease of the hardness experimentally observed at small lattice periods can be due to two effects.

(1) For $\lambda_1$ smaller than about 15–20 times the Burgers vector $b$ the repelling mirror forces induced by the strain in the layer of stronger materials on both sides of layer M(1) begin to cancel each other out (these forces have opposite signs with respect to each other) and, therefore, enhancement of the strength decreases.
(2) The other effect is the roughness of the interface due to interdiffusion during the preparation. This effect was discussed in a number of papers (see, e.g., Refs. 205 and 223–225). Chu and Barnett have shown that an interface roughness of about 1 nm will cause a strong decrease in hardness and it probably dominates the experimentally observed softening for $\lambda < 5$–7 nm.[225] Recent experimental data on superlattice with high immiscibility, which form sharper interfaces, support this conclusion.[226–229] In nonisostructural epitaxial Mo/NbN and W/NbN superlattices only a relatively small decrease of the hardness was found for a superlattice period of $\leqslant$2–3 nm. Even for the smallest period near 1 nm the hardness of the heterostructures was significantly higher than that for the rule of mixture.

TiN/AlN superlattices of equal TiN and AlN thickness are interesting because of the ''template effect'' that is imposed on the hexagonal wurzite structure of AlN which changes to the high pressure cubic phase when the superlattice period decreases to $\leqslant$3 nm.[230,231] The hardness increased to 40 GPa for that superlattice period. Such a template effect also appears in TiN/AlN nanocomposites,[232–234] which will be discussed in Sec. IV B. Some other examples of the template effect which include TiN/NbN, TiN/CrN, and TiN/ $CN_x$ heterostructures were discussed by Sproul.[214,215]

In a remark added in proof, Koehler mentioned that the ideas described in his paper would also be valid if one of the layers is amorphous. In spite of that, the researchers were studying only epitaxial and, later on, polycrystalline heterostructures. Recently, several papers appeared in which one of the layers consists of, e.g., amorphous $CN_x$ the other of a transition metal nitride such as TiN[214,217–219] or ZrN.[214,216] However, with decreasing layer thickness the layered structure vanished and a nanocrystalline composite structure appeared.[214,216–219] Such films also show a high hardness of about 40 GPa.

Hardness of about $\geqslant$40 GPa was reported by Holleck and co-workers also for various multilayers consisting of TiN, TiC, $B_4C$ (more exactly, $B_{13}C_3$), and metastable TiBC and TiBN solid solutions.[235,236] The basic idea of Holleck was similar to that of Koehler, i.e., to increase the strength of the coatings by introducing a large number of coherent interfaces.[159,237–238] However, Holleck was following a more practical approach in which the emphasis was on the selection of materials for practical applications. Such multilayers are presently used predominantly to match coating properties to the substrate and to the machining conditions.[235,236] Enhancement of the hardness is only one of many aspects in the improvement of coating performance including high temperature toughness, mechanical stress, adhesion, friction coefficient, and others which are important for machining applications.[1–3,78]

Heterostructures as well as multilayers are prepared by plasma PVD techniques, such as sputtering or vacuum arc evaporation, from two different material sources. The majority of researchers uses reactive sputtering where either the two sources are periodically switched on and off (e.g., using shutters[222]) or the substrates are mounted on a rotating turntable (see, e.g., Refs. 216–218). Because plasma PVD operates at low pressure where the sputtered or evaporated material is transported from the source to the substrate without scattering in the gas phase, complex planetary motion of the substrates is necessary in order to coat nonplanar substrates.

In summary, great progress has been achieved in the preparation and understanding of the hardness and strength enhancement in heterostructures. Also, the application of the heterostructures[239,240] and multilayers[235,236] for cutting tools has been fairly well developed. Cutting tools coated with multilayers with superior properties as compared to tools with single layer coatings are available from several companies.

## B. Nanocrystalline composite materials

### 1. Concept for the design

Grain boundary hardening [see Eq. (3)] and the discussion of the Hall–Petch relationship could in principle yield superhard materials if grain boundary sliding could be avoided in hard polycrystalline materials with grain sizes in the few nanometer range. Based on an understanding of these mechanisms one can expect that appropriate design of nanocomposites with strong grain boundaries such as nanocrystalline/amorphous ($nc$-/$a$-)[6,241–246] or nanocrystalline biphase

(*nc*-/*nc*-) composites with coherent grain boundaries[77] (similar to that suggested for the multilayers[5,237]) can avoid grain boundary sliding. Thus, the hardness of such a material should continue to increase even for grain sizes below 6–10 nm. When designed of strong materials with a hardness of $\geqslant$20 GPa, essentially all such nanocomposites should reach a superhardness of $\geqslant$40 GPa.[6,77,241–243,247,248] Even the hardness of diamond represents an increase by only a factor of 3–4 compared with conventional hard materials, such as transition metal nitrides, carbides, and borides.[159]

However, one has to keep in mind that the appearance of grain boundary sliding depends on the temperature (see the literature on deformation mechanism maps[9,192–198]). Thus, sliding, which is absent at room temperature, may occur at elevated temperatures of $\geqslant$800 °C, which is reached, e.g., at the edge of cutting tools. For these reasons, the behavior of the material's properties at elevated temperature (e.g., hot hardness and structural stability) represents an important issue in the field of nanocomposites and it has to be investigated in great detail.

An idealized microstructure of such a composite suggested in Fig. 1 of our earlier paper[6] is based on isolated nanocrystals (e.g., *nc*-TiN) imbedded in a thin matrix (e.g., *a*-$Si_3N_4$). Alternatively, one might also evoke an interwoven biphase system as observed by Milligan *et al.* for *nc*-Au/*a*-Si (see Fig. 6 in Ref. 249) or a bicontinuous two-phase system. In *nc*-TiN/*a*-$Si_3N_4$ nanocomposites which were investigated in some detail thus far, detailed high resolution transmission electron microscopic study revealed only isolated nanocrystals imbedded within the amorphous matrix,[245,246] in agreement with the nanostructure suggested.[6] In order to form such a biphase system, both materials must be immiscible (i.e., they must display thermodynamically driven segregation during deposition) and the cohesive energy at the interface between the both phases must be high.[6,241–244] Last, but not least, the amorphous (or a second nanocrystalline) phase must possess high structural flexibility in order to accommodate the coherency strain without forming dangling bonds, voids, or other flaws. Both materials should be refractory so that the operational temperature of the tools will be smaller than half of the melting or decomposition temperature. In this case the nanostructure would be stable and grain boundary sliding may be avoided.

It is important to note that, although the strengthening caused by the decreasing dislocation activity due to decreasing crystallite size finally reaches a saturation due to the absence of dislocations in ultrasmall nanocrystals, the strength and hardness of such a material may still increase upon further decrease of the crystallite size in the range of $\leqslant$10 nm when another strengthening mechanism becomes dominant. In the absence of dislocations and grain boundary sliding the nanocomposites show brittle behavior which means that the fracture strength (and hardness) is proportional to the elastic modulus of the material. This behavior has been confirmed in several nanocrystalline superhard composites made of different materials.[6,241–244] The fracture stress of such a material should then be determined by the critical stress for the growth and deflection of microcracks [see Eq. (4)]. The size of microcrack $a_0$, i.e., of a possible flaw and voids, is in a well compacted material always smaller than the size of the nanocrystals, $a_0 \leqslant d$. With this simple model in mind, many mechanical properties of nanocomposites that were studied so far can be fairly well explained. However, one has to keep in mind that this model is very simplified and our understanding of nanocomposites is in its infancy. The mechanism of the toughening of nanocomposite ceramics is probably much more complex, including switching from intergranular cracking to transgranular cracking and fracture surface roughening.[250] which provides ample possibilities for crack deflection, meandering, and plastic zone shielding.

The obvious first (but by far not the only one) choice of such a *nc*-/*a*- system that meets the above discussed criteria for achieving superhardness is straightforward: Many transition metals $M_nN$, such as Ti, Zr, Hf, V, Nb, Ta, and Cr form stable, refractory, hard nitrides[4,251–254] which crystallize upon deposition even at relatively low temperatures of $\geqslant$100 °C.[159,251,252] Silicon nitride, on the other hand, grows amorphous even at 1100 °C and it possesses the desirable structural flexibility due to the fourfold coordination of silicon combined with the threefold coordination of nitrogen. TiN–$Si_3N_4$ is immiscible up to a relatively high temperature of 1000 °C.[4,251,253,254] Moreover, silicides of transition metals are refractory materials with a high Gibbs free energy of formation comparable to that of borides and carbides, and have large compositional flexibility.[88] Therefore, the *nc*-TiN/*a*-$Si_3N_4$ interface is expected to be sufficiently strong in order to avoid grain boundary sliding. A simple thermodynamic estimate[242] shows this similarly applies to the majority of the transition metal nitrides mentioned above.[4,77,254–256] In order to reach superhardness, the concentration of the $Si_3N_4$ phase should be about 16–23 mol % (the reason will be discussed later).

An even better choice of the amorphous (or nanocrystalline) phase in combination with a nanocrystalline transition metal nitride would be boron nitride because boron atoms can be three- and fourfold coordinated and the B–N bond is stronger than the Si–N one. Because of the great stability and the compositional and structural flexibility of borides,[88] the interface should also be strong. However, the problem in the preparation of the *nc*-TiN/BN nanocomposite is associated with formation of the soft hexagonal phase h-BN which results in a strong decrease of the hardness of the composite when the nitrogen content is increased from that of the composition of TiN/$TiB_2$ towards that of TiN/$BN_x$.[257] This problem was solved recently and superhard *nc*-TiN/BN nanocomposites with hardnesses between 60 and 80 GPa were reported.[77,258] Because silicon dissolves in many metals, the choice of boron nitride, aluminum nitride, and other materials as the grain boundary material offers potential advantages with respect to many applications in, e.g., machining.

### 2. Preparation of the nanocomposites

In order to assure that thermodynamically driven segregation and formation of the nanostructure occur during deposi-

tion the activity of nitrogen must be sufficiently high and the substrate temperature relatively low, yet high enough to allow diffusion during film growth. For stable transition metal nitrides such as TiN and others this applies for nitrogen pressures above about 1 mbar and temperatures below about 600–700 °C.[4,6,241–243] A similar estimate shows that the segregation should be much stronger in the TiN/BN and many other $M_nN$/BN systems compared to the $TiN/Si_3N_4$ one.[77] Therefore, the appropriate preparation technique should assure high nitrogen activity and sufficient activation energy for the thermodynamically driven segregation of the phases to occur at a temperature of 400–550 °C which is compatible with the majority of engineering substrate materials.

Activated chemical or physical vapor deposition techniques such as plasma CVD and PVD are most suitable. Because plasma CVD usually operates at a higher pressure of about 1–5 mbar whereas a lower pressure of $\leqslant 10^{-3}$ mbar is used in plasma PVD, plasma CVD was used in the initial work.[6,241–244,259] It also provides somewhat better flexibility regarding the choice of the $nc$-$M_nN/a$-$A_xN_y$ system. However, plasma CVD still suffers from problems of scaling from a small experimental reactor to large scale production units. Also, the use of volatile transition metal halides as sources of those metals makes it less attractive for industrial applications because of the problems associated with the corrosive nature of the chlorine to the vacuum pumps and the hydrophilic nature of the deposits at the reactor walls and in the vacuum tubings. The use of organometallic precursors in plasma CVD results usually in the incorporation of large amounts of carbon in the deposit due to the poor chemical selectivity of the process. For these reasons, a combined plasma PVD and CVD technique[77,258,260] or reactive sputtering[261] is more appropriate for future industrial applications but plasma CVD will probably remain the preparative tool for basic studies on a variety of $nc$-/$a$- and $nc$-/$nc$- systems. Both high frequency (HF)[6,241–244] and direct current (dc)[76,77,259,262,263] glow discharges were used for the deposition, yielding essentially the same coatings if the ion bombardment were kept relatively low. If the discharge is operated in the abnormal glow regime,[264–266] the negative glow covers the whole surface of the cathode and follows the shape of a curved surface. This applies also to the HF discharge at sufficiently high power density where the high impedance of the space charge sheath near the electrode has a similar function as that in the abnormal dc glow.[267,268] In such a way, nonplanar substrates mounted at the electrode can be uniformly coated. As already mentioned in Sec. IV A plasma PVD techniques which operate at a much lower pressure of the order of $\leqslant 10^{-3}$ mbar require planetary motion of the substrates.

TiN prepared from $TiCl_4$ usually suffers from a relatively large chlorine content, which for thermal CVD films deposited at 1000 °C, can approach almost 1 at. % and is much higher in films prepared by means of plasma CVD at lower temperatures.[269,270] It was shown that the chlorine content of TiN deposited at 500 °C can be significantly reduced by increasing the discharge current density.[271,272] Using this principle and a large excess of nitrogen and hydrogen, $nc$-TiN/$a$-$Si_3N_4$ films deposited at 500–550 °C contain $\leqslant$0.5 at. % chlorine, which is fairly tolerable. The same also applies to other nitrides.

Plasma PVD has the advantage of being a halogen-free process, but it is more difficult to achieve the sufficiently high chemical activity which is needed for the phase separation and formation of the nanocomposite. This results in the deposition of homogeneous metastable solutions, such as $Ti_{1-x}Al_xN$ (Refs. 273–275) or Ti(BN).[15,152,276] Other authors have found phase segregation with the formation of binary nanocomposite phases of TiN and $TiB_2$ in Ti–B–N coatings with relatively little nitrogen.[257,277–284] From the published data it appears that higher substrate temperature and bias promote phase segregation which results in higher hardness. The hardness of the films depended on the composition, showing a maximum for a composition of about $Ti_1B_{0.6-1}N_{0.5}$ where the coatings had a very fine, almost isotropic, nanocrystalline microstructure.[279,280] The value of the maximum hardness depended on the substrate temperature and the negative basis applied. For $T_{\text{substrate}}$ of 300–400 °C, ion energy of 126 eV, and a ratio of the ion to atom flux to the substrate of 0.7 the hardness reached about 50 GPa or slightly more for nitrogen content of $\leqslant$15 at. %. In general, the hardness as a function of the composition did not follow the rule of mixture (defined in Sec. I) but displayed a maximum at a given composition where the microstructure of the films was very uniform (no columnar growth) and the crystallite size was a few nm. With increasing nitrogen content, when the h-BN phase was formed, the hardness of the films strongly decreased to 15–20 GPa for an overall composition of $TiB_2N_2$.[257,283,284] This decrease was attributed to the formation of soft h-BN.

If, however, much higher temperature, high plasma density, and negative bias were used, the formation of the h-BN was suppressed and superhard $nc$-TiN/BN nanocomposites were obtained by a combined plasma PVD and CVD.[77,258,260] This example shows the importance of the plasma parameters for achieving the above discussed thermodynamically driven segregation. As in all other systems, the optimum hardness and morphology are achieved at a BN phase concentration of about 20 mol %. There is no sign of any $TiB_x$ or h-BN seen in the XRD of the films. The BN phase is either amorphous or ''cubic'' or a mixture of both. (This is difficult to see in XRD due to the relatively small fraction of that phase and the small x-ray scattering factor of boron compared to that of Ti, which scales with the atomic number.) In contrast to the softening of the material with the nitrogen content increasing from that of TiN/ $TiB_2$ towards the TiN/BN observed by Mollard and co-workers,[257,283,284] the hardness of these $nc$-TiN/BN coatings with an average TiN crystallite size in the range of a few nm exceeds 60 GPa.[77] Figure 2(c) shows a more recent example of the measurements on new $nc$-TiN/BN coatings with hardness in excess of 60 GPa. Even taking a sober view with regard to the meaning of the measured values of hardness in this range (see Sec. II A), a comparison of the indentation curve in Fig.

2(c) with that of diamond [Fig. 1(b)] shows that the hardness of these coatings approaches that of diamond. Most convincing is the small area of indentation between the loading and unloading curves which is a measure of the energy of the plastic deformation. These coatings are deposited in an industrial unit which allows one to simultaneously coat a larger number of cutting tools[77,258,260] made of, e.g., ''hard metal'' (Co-cemented WC) without any noticeable problems regarding the adhesion. Scratch tests using a Rockwell diamond tip (with a speed of 10 mm/min and load increase of 1.5 N/s) and acoustic detection of the delamination with a subsequent measurement of the delamination under a microscope reveal an adhesion of $\geqslant$70 N which is fairly good for applications.

Several researchers have also reported an increase of the hardness of various nanocomposites if they were, after deposition at a relatively low temperature, postannealed. This has been reported for (TiZr)N coatings deposited by sputtering[285] or vacuum arc evaporation[286–288] and attributed to spinodal decomposition of the as deposited homogeneous alloy. Gissler and co-workers[279–280] deposited a Ti/BN multilayer which was initially soft ($H_V$ about 10 GPa) but after annealing at $\geqslant$400 °C the hardness increased to more than 40 GPa. Similarly (TiAlSi)N coatings of composition $(Ti_{0.05}Al_{0.44}Si_{0.06})N$ prepared by vacuum arc evaporation at a deposition temperature of $\leqslant$600 °C (Ref. 289) show an increase of hardness upon subsequent annealing.[258,260]

To summarize: The simple thermodynamical consideration shows that thermodynamically driven segregation, which is a prerequisite for the phase separation necessary for nanocomposite formation, should occur in a large number of systems, particularly those consisting of nitrides. (It can be easily estimated that the same applies also to many oxides and carbides.) The formation of a nanocomposite requires high plasma density and temperature as was demonstrated for various systems. To achieve superhardness a certain ratio of the fractions (typically close to 80:20 mol %) of the two phases is necessary in order to provide the driving force for the segregation and resultant formation of the nanostructure (Ref. 263).

### 3. Properties of *nc*-$M_nN$/*a*-$Si_3N_4$ composites

To achieve superhardness a certain concentration ratio of the two phases (mentioned above) is necessary. This has been shown in some detail for *nc*-TiN/*a*-$Si_3N_4$,[241,242,245,246,259] *nc*-$W_2N$/*a*-$Si_3N_4$,[243] and *nc*-VN/*a*-$Si_3N_4$, (Refs. 6 and 244) nanocomposites which reach the highest hardness of $\approx$50 GPa when the concentration of the *a*-$Si_3N_4$ phase is about 17–23 mol %. This is accompanied by a characteristic development of the nanostructure. The typical columnar structure of plasma deposited TiN vanishes with increasing additions of *a*-$Si_3N_4$ and an isotropic finely grained nanostructure develops when a concentration of 17–23 mol % is achieved.[243,245,246] Andrievski reported a similar evolution of the microstructure of $TiB_2$/$TiN_x$ coatings where a finely grained isotropic nanostructure and high hardness of $\geqslant$40 GPa were found for a composition of 75 mol % $TiB_2$/25 mol % TiN (see Fig. 1 in Ref. 287). Gissler and co-workers[279,280,284] reported the maximum hardness of their Ti–B–N coatings for a composition of about $TiBN_{0.4-0.6}$ where also a finely grained nanostructure with a crystallite size of a few nm was found. The highest hardness of the *nc*-TiN/BN coatings is also achieved when the BN fraction is around 20 mol %.[77,258]

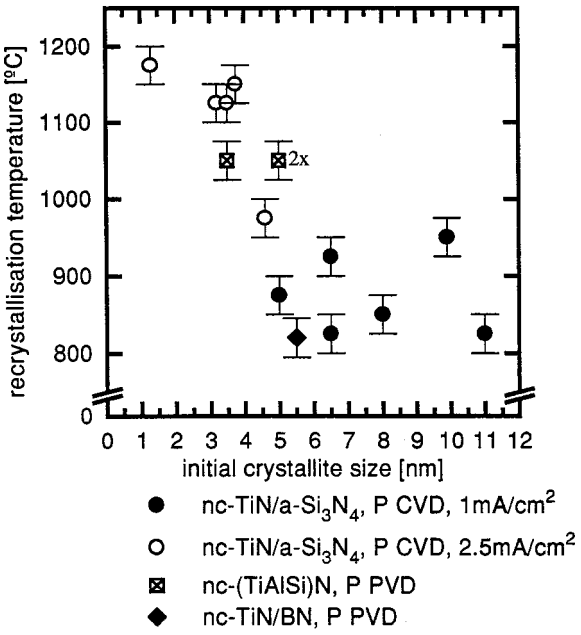


FIG. 3. Recrystallization temperature of *nc*-TiN/*a*-$Si_3N_4$ and (TiAlSi)N nanocomposites vs the average crystallite size. The hardness of the coatings remains unchanged up to recrystallization.

In earlier work on *nc*-TiN/*a*-$Si_3N_4$ (Refs. 241, 242, 245, and 246) and on *nc*-$W_2N$/*a*-$Si_3N_4$ and *nc*-VN/*a*-$Si_3N_4$,[6,243,244] this maximum of hardness correlated with a minimum crystallite size of about 3–4 nm for a $Si_3N_4$ content of 17–23 mol %. This has been attributed to the percolation threshold[290] when the structurally flexible and less polar $Si_3N_4$ wet the surface of the TiN nanocrystals thus decreasing the Gibbs free energy of the system by the formation of a strong interface[6,77,243–245,263] This may also answer the question as to why these systems segregate into the nanocrystalline composite and not into a coarsely grained one which should be, in general terms of thermodynamics, more stable (see Ref. 263 for further discussion). In a more recent work, where a more intense ion bombardment was applied during deposition at a higher discharge current density of $\geqslant$2.5 mA/cm$^2$, the crystallite size showed a monotonous decrease with increasing $Si_3N_4$ content, but the maximum hardness was again obtained for a content of about 20 mol %.[77,262,263]

Although the available data on other systems do not allow one to make any final conclusion, there seems to be a clear tendency in all these systems to spontaneously form a superhard nanostructure due to phase segregation during deposition or due to spinoidal decomposition upon postannealing if the composition is close to the percolation threshold and the conditions are such as to allow segregation to occur. The fact

that the systems form a nanocomposite instead of a coarsely grained segregated two-phase system suggests that there must be some kind of a stabilizing effect for the nanocomposites, possibly due to a strong interface. The coherency strain which is the origin of disperse order in nanocrystalline metals[291,292] can hardly explain the surprisingly high thermal stability of these nanocomposites (see below). This is one of the challenging questions to be clarified in the near future.

Figure 3 shows the dependence of the recrystallization temperature of *nc*-TiN/*a*-$Si_3N_4$ nanocomposites on the crystallite size determined from the XRD pattern by means of Warren–Averbach analysis.[262,263] (Warren–Averbach analysis allows one to separate the contribution to Bragg peak broadening due to the finite crystallite size and random stress.) The crystallite size was controlled by the composition of the films and/or by the ion bombardment as mentioned above. The films were annealed under 5–10 mbar of forming gas ($\sim$95% $N_2$/5% $H_2$) for 30 min. The hardness of the films did not change up their respective recrystallization temperatures which are determined by the corresponding crystallite sizes in Fig. 3. Upon recrystallization the hardness decreased. This clearly shows that the stability of the hardness is controlled by the stability of the nanostructure and it is not influenced by the fairly small biaxial compressive stress of $\leqslant$0.4 GPa.[262,263]

One notices that the recrystallization temperature increases with decreasing crystallite size. Important is the fact that the hardness of the films in this series correlates with the crystallite size in the way reported earlier[241,242,245,246] only for the low ion energy bombardment in the HF discharge but it decreased monotonously with increasing $Si_3N_4$ content for films deposited at the cathode of the dc discharge at $\geqslant$2.5 mA/cm$^2$. This means that the stability of the nanostructure is determined by the crystallite size irrespective of the hardness. An annealing temperature of 1100 °C corresponds to 0.76 $T_{\mathrm{dec}}$ of the decomposition temperature of $Si_3N_4$.[254] Thus, the absence of recrystallization (Ostwald ripening[293,294]) due to slow diffusion seems to be unlikely because the diffusion is solids strongly increases at $T \geqslant 0.5T_{m,\mathrm{dec}}$.[295] Also, measurements of the diffusivity in the TiN/$Si_3N_4$ and TiN/Si systems support this conclusion (see, Refs. 74 and 262, and references therein). The fact that the (TiAlSi)N nanocomposites fit in the data of Fig. 3 lends further support to the hypothesis that such behavior may be a universal phenomenon.[262,263]

It will be important to perform such study on other nanocomposites in order to see if such behavior is a general phenomenon. An important parameter to be considered is the coherence of the interface between the two phases. Coherence stress and composition gradients at the interface can influence the diffusion coefficient[296,297] and also change the melting point.[297,298–300] Both an increase and a decrease of the diffusion coefficient and $T_m$ are possible depending on the exact conditions and properties of the system.[296,297] The increase of the stability up to $\geqslant$1100 °C for the small grain size nanocomposites in Fig. 3 correlates with a similar increase of the random stress determined from Warren–Averbach analysis.[263] Therefore it may be a possible explanation. However, the strong increase of the recrystallization temperature shown in Fig. 3 seems to be too high to be explained by such an effect. Therefore, one should also consider the possibility of the stabilization of the interface due to a quantum confinement phenomenon as was hypothesized recently.[77,243] However, more likely appears to be a stabilization of the nanostructure in a two- or three-phase system which undergoes a strong, thermodynamically driven segregation. Such a segregation causes a reduction of the grain boundary specific energy which results in a metastable state which is stable with respect to a variation of its total grain boundary area. Such a two-phase system is stable against recrystallization up to a high temperature where the solubility increases (see Ref. 263 and references therein).

The high thermal stability of the smallest grain size nanocomposites is very important from the practical point of view, because it will allow one to tailor the properties of the coatings to the given application. As mentioned in Sec. I, the temperature at the edge of the cutting tool can reach a temperature in excess of 800 °C and room temperature high hardness is only one of many properties to be optimized. The choice of the small grain size of $\leqslant$4 nm will provide the coatings with sufficient thermal stability against recrystallization. The question however that remains is whether these coatings will also be stable against oxidation at such high temperatures. Data available so far for the *nc*-TiN/*a*-$Si_3N_4$,[242] *nc*-(TiAlSi)N,[289] and *nc*-TiN/BN, (Refs. 77 and 258) coatings showed that they are oxidation resistant in air up to $\geqslant$800 °C like the $Ti_{1-x}Al_xN$ coatings. A potentiostatic polarization measurement on the $Ti_{0.5}B_{0.5}N_{0.5}$ coatings showed that they are, under such conditions, more oxidation resistant than TiN and even more so than stainless steel.[278] A systematic investigation of the oxidation resistance at high temperatures as a function of the grain size is therefore needed.

Relatively little work has been published so far regarding the performance of the coatings in machining tests. The superhard Ti–B–N coatings from the ''zone 4'' of the Ti–B–N phase diagram (i.e., $TiB_2/TiN_x$) displayed a shorter lifetime than TiN (probably due to a lower value of the adhesive strength) but higher flank wear (see Ref. 279, and references therein). The expectation that the h-BN phase would provide coatings with self-lubricant properties was also not confirmed.[283] However, implantation of carbon into such coatings reduced the coefficient of friction significantly from 0.8 for the Ti–B–N coatings to about 0.2 for the carbon implanted ones.[301] The $(Ti_{0.50}Al_{0.44}Si_{0.06})N$ nanocomposite coatings have only slightly lower adhesion (of about 60–70 N) than TiAlN (60–80 N) and TiN (75–95 N) which does not affect their performance in cutting tests. Compared with the uncoated WC–Co indexable inserts and those coated with TiN and TiAlN, the $(Ti_{0.5}Al_{0.44}Si_{0.06})N$ coatings showed the smallest flank wear.[289] More recent data on the cutting performance of these and *nc*-TiN/BN are very promising.[258]

### 4. Other superhard nanocomposites

Hultman and co-workers reported on the formation of nanocomposites due to spinodal decomposition $Ti_{1-x}Al_xN$ ($0 \leqslant x \leqslant 0.4$) at elevated temperatures during deposition.[232–234] The template effect caused the AlN (or AlN-rich) phase to crystallize in the metastable, high pressure NaCl cubic structure. No hardness was reported in these papers. A similar template effect was observed also by Sproul, Chung, and co-workers during the deposition of $TiN/CN_x$ (Refs. 217–219) and $ZrN/CN_x$ (Ref. 216) heterostructures at a relatively low temperature of $\leqslant$200 °C. As mentioned in Sec. IV A, the hardness of the superlattice increased to about 40 GPa when the superlattice period decreased to 4 nm. However, upon a further decrease of the period of 2 nm the layered structure vanished and a superhard $TiN/CN_x$ or $ZrN/CN_x$ nanocomposite formed. XRD showed a (111) film texture and high resolution transmission electron micrographs revealed that the material consisted of a *nc*-$M_nN/CN_x$ nanocomposite (M=Ti and Zr) with CNx pseudomorphic growth on the $M_nN$ template. The formation of these nanocomposites was attributed to ion bombardment induced mixing during film growth. However, a critical reader will ask why the mixing should lead to the formation of a nanocomposite if TiN and TiC as well as ZrN and ZrC form a stable solid solution within the whole range of the composition.[302,303]

It is interesting to compare these $TiN/CN_x$ heterostructures and composites prepared by reactive sputtering at a relatively low pressure of about 0.01 mbar and temperature of $\leqslant$200 °C with the results obtained by plasma CVD at significantly higher pressure of 1–5 mbar and temperature of 560 °C.[6] Because carbon can substitute for nitrogen in the TiN crystal lattice, $TiC_xN_{1-x}$ forms a homogeneous solid over the whole range of $0 \leqslant x \leqslant 1$. The higher deposition temperature and high activation energy provided by the intense glow discharge plasma during plasma CVD resulted in the formation of a well mixed titanium carbonitride, $TiC_xN_{1-x}$. The hardness of the films plotted versus the composition parameter $x$ did not show any extremum, but followed monotonously the rule of mixture, increasing from a hardness of TiN of about 20 GPa to that of TiC of nearly 40 GPa.[6]

In course of their studies of the multilayer coatings[159,236—238] Holleck and co-workers also reported on $TiB_2$/TiC coatings whose hardness approached 40 GPa for a composition of 20 mol % $TiB_2$/80 mol % TiC.[304] These coatings also showed a high hot hardness.

Knotek[305] prepared ''superstoichiometric'' carbides, $MC_{1+x}$, by reactive sputtering which, in fact, consisted of nanocrystals of stoichiometric carbides imbedded in a *a*-C:H matrix. With increasing excess $x$ of the carbon, the hardness of the films increases, reaches a maximum of about 40 GPa and, afterwards, decreases again upon a further increase of $x$ in a similar manner as in *nc*-MnN/*a*-$Si_3N$ nanocomposites. Voevodin and Zabinski reported recently a maximum hardness of *nc*-TiC/*a*-C films with a total carbon content of 65 at. 5% to be 32 GPa.[306,307] Although these composites are not superhard, the high toughness of 70 N and low coefficient of friction of 0.15 (Ref. 307) are important for various wear applications. The superhard amorphous $B_4C$ which was briefly discussed in Sec. III C can be regarded as a nanocomposite consisting of boron quasicrystals.

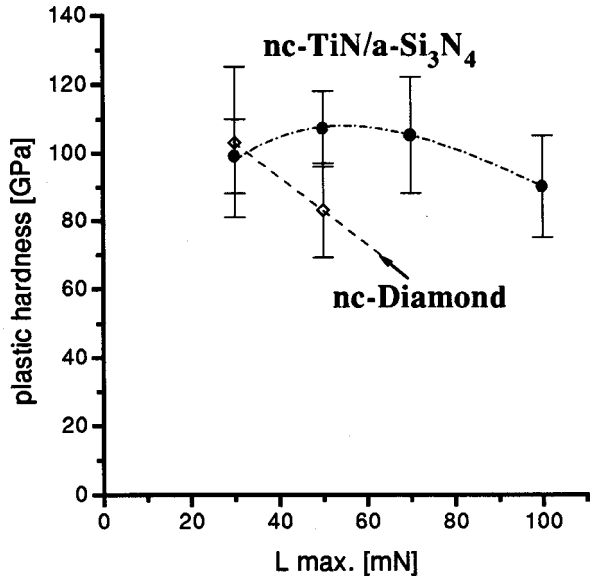


FIG. 4. Hardness of a 3.5 $\mu$m thick *nc*-TiN/*a*-$Si_3N_4$ coating deposited on stainless steel in comparison with the hardest single phase nanocrystalline diamond 1.5 $\mu$m thick film (Ref. 109) plotted vs the maximum applied load.

The significant limitation regarding the applicability of these carbon containing superhard nanostructured materials is the high solubility of carbon in ferrous alloys (however, not in Al alloys) and the low thermal stability of transition metal and boron carbides against oxidation in air. The stability of $B_{13}C_3$ is limited by the oxide's low melting point of about 460 °C, which allows fast diffusion of oxygen and results in oxidation of the film. In the case of *a*-C:H and $CN_x$ containing composites one has to keep in mind that these carboneous materials decompose at a temperature of 300–500 °C. Therefore, all these materials may find application only at relatively low temperatures.

### 5. Hardness of diamond achieved

After writing this review but before it was published, the hardness of the *nc*-$TiN/SiN_x$ nanocomposites was able to be increased further, reaching a value of 105 GPa.[82] This was achieved by an appropriate balance between the deposition rate, temperature, and ion bombardment. Figure 4 shows an example of the hardness of the coating measured in comparison with that of single phase nanocrystalline diamond[109] versus the maximum applied load. The nanocrystalline diamond was the hardest diamond sample that we could obtain from various laboratories, the hardness of the others varied between about 70 and 80 GPa or less. One can see that the hardness of the *nc*-$TiN/SiN_x$ coatings is at least as high as that of the best nanocrystalline diamond. In order to carefully check and support these results, the size of the remaining indentation was measured by means of scanning electron microscopy (SEM) and the hardness calculated according to the standard Vickers procedure.[7] For a load of 100 mN a hard-

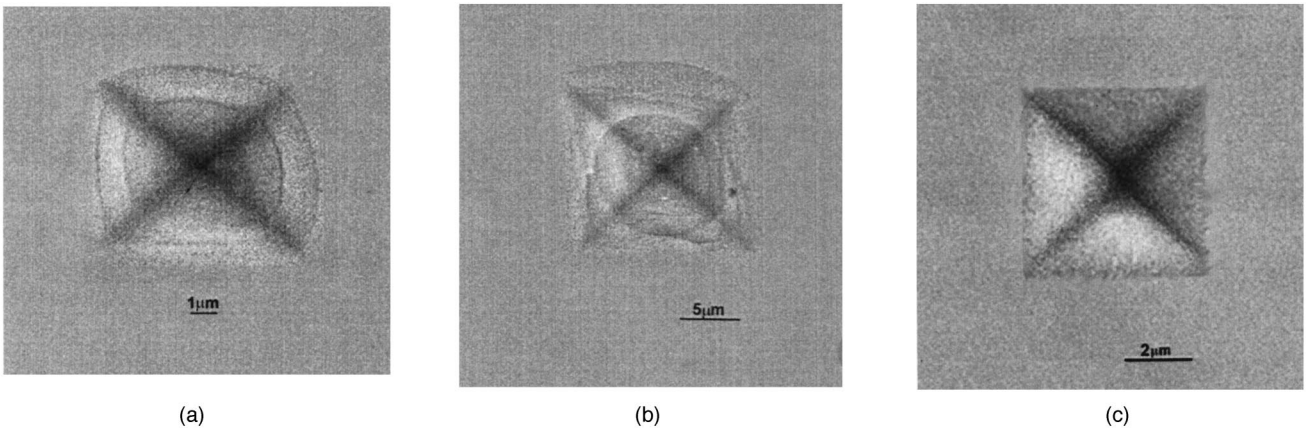


FIG. 5. SEM micrographs of the indentations remaining in the *nc*-TiN/$SiN_x$ coatings: (a) 3.5 $\mu$m thick coating with an applied load 500 mN; (b) the same coating as in (a) but with a load of 1000 mN; (c) 10.3 $\mu$m thick coating after indentation with a load of 1000 mN.

ness of $\geqslant$91 GPa was obtained, in agreement with the indentation measurement. Also, the values of universal hardness of about 18–20 GPa and elastic moduli of 450–500 GPa are similar for *nc*-TiN/$SiN_x$ coatings and the diamond. The indentation curves showed a close similarity in the areas corresponding to the energy of the plastic deformation. An enhancement of the measured hardness due to compressive biaxial stress in the films (as discussed above) can be ruled out because the stress is less than 0.4 GPa and the hardness remains unchanged after 0.5 h annealing up to the recrystallization temperature (see Fig. 3).[262,263]

Figure 5 shows examples of SEM micrographs of indentations at high loads. In the case of the 3.5 $\mu$m thick coating and a load of 1000 mN the coating is pressed almost 5 $\mu$m deep into the soft steel substrate. Yet only circular, but no radial, cracks are seen. In the case of a somewhat softer but much thicker (10.7 $\mu$m) coating, shown in Fig. 5(c), neither radial nor circular cracks are seen. This shows that the toughness of these coatings is very high, and not measurable with the conventional indentation technique.[71,79–81]

The hardness of about 105 GPa reported here for the *nc*-TiN/$SiN_x$ coatings is about a factor of 4–5 higher than that of TiN and about a factor of 5–5.5 higher than that of $Si_3N_4$. This is within the usual range of strengthening of engineering materials by appropriate tailoring of their microstructure (see above). Therefore the superhardness of these nanocomposites in the range of the hardest diamond is a simple consequence of the appropriate design of their nanostructure and of the TiN/$SiN_x$ interface which avoids grain boundary sliding. The experimental results clearly indicate that this is a result of an interplay between the deposition rate and the temperature as well as appropriate dosing of the ion bombardment. More work is needed to quantify this relationship and to identify the exact nature of the interface. Our preliminary results indicate that it consists mainly of Ti–Si bonds and, in some cases also of $TiSi_2$ precipitates.[82]

The high elasticity and toughness are also a logical consequence of the nanostructure: The high elasticity follows from the absence of dislocation activity in $\leqslant$10 nm small nanocrystsals. The plastic deformation observed under the indentation is due to a brittle fracture, such as is observed in glasses. The high toughness can be qualitatively understood in terms of ample possibilities for the deflection, meandering, and plastic zone shielding in the randomly oriented nanocomposite, as well as the high critical stress $\sigma_C \propto d^{-0.5}$ which is needed to initiate the propagation of a nanocrack, a flaw which may be present within the thin grain boundary matrix after deposition. We refer the reader to a forthcoming paper for further details.[82,263]

## V. CONCLUSIONS

Intrinsic superhard materials include diamond, cubic boron nitride, and other materials from the C–B–N triangle, boron carbide and boron suboxide. Diamond and probably also cubic boron nitride are metastable polymorphs. Therefore, they are prepared either by high temperature high pressure transformation catalyzed by appropriate metal or as coatings for an appropriate substrate by kinetically controlled activated deposition from the gas phase. The great progress which has been achieved in the diamond deposition process during the last 10 years still results in rather limited applications of it as hard coatings on cutting tools because of the high solubility of carbon in ferrous alloy and various other materials. The deposition of cubic boron nitride requires intense ion bombardment of the growing film during deposition in order to reduce the concurrent formation of the stable hexagonal soft h-BN. This results in large compressive stress which limits the practically achievable thickness of *c*-BN coatings. For these reasons only *c*-BN based ceramics find wider application. C–B–N superhard coatings are emerging as an interesting class of new superhard materials.

Most promising superhard materials for a wide range of applications appear to be the nanostructured materials, such as heterostructures and nanocomposites. Great progress in the preparation of heterostructures and understanding of their properties has been achieved during the last 25 years. Heterostructures and multilayers are finding increasing numbers

of applications as wear resistant and protection coatings. Superhard nanocomposites are at the beginning of their development. The last few years have shown that the concept for their design should be valid for a large number of different ternary and quaternary materials. This opens up many possibilities for tailoring the desirable properties, such as hot hardness, toughness, adhesion, and compatibility with the substrate and with the material to be machined. The fast growing number of research groups working in this field will surely result in fast progress in the near future. There are many questions remaining regarding the nature of the interfaces which hinder grain boundary sliding in nanocomposites with grain sizes of 2–10 nm, and the formation and the high temperature stability of the nanostructure.

More recently *nc*-TiN/$SiN_x$ nanocomposite coatings with a hardness of 105 GPa, i.e., equal to the hardest diamond, were prepared. Future research will be directed towards the understanding of these materials as well as to their industrial applications. The world of nanocrystalline materials is fascinating, not only with respect to their mechanical properties discussed here, but also for their optoelectronic and magnetic properties which are receiving the growing interest of scientists.[248,308–311]

*Note added in proof:* Our more recent investigation into the ultrahard nanocomposites with $H_V \geqslant 100$ GPa have shown that the grain boundary matrix is substoichiometric $SiN_x$, and it can even be like $TiSi_2N_x$. Therefore we prefer to write it as *nc*-TiN/SiN*x*. See Ref. 82 for forthcoming details.

## ACKNOWLEDGMENTS

The author would like to thank his co-workers for their enthusiastic collaboration and his colleagues and friends, Professor Li Shizhi, and Professor J.-E. Sundgren, and many others for illuminating discussions. Special thanks are due to his wife, Dr. Maritza G. J. Vepřek-Heijman, for her great help with the literature search and critical reading and corrections of the manuscript. Thanks also to Dr. D. M. Gruen and Dr. A. R. Krauss for providing him with the hardest *nc*-diamond films. Partial financial support of this work by the German Science Foundation (DFG), by the Bavarian Ministry for Education and Science and by the NATO SFP Programme No. 972379 are gratefully acknowledged.

[1]W. Schedler, *Hartmetall für den Praktiker* (VDI, Düsseldorf, 1988).
[2]*Metals Handbook*, 10th ed., edited by J. R. Davis, P. Allen, S. R. Lampman *et al.*, (ASM International, Metals Park, OH, 1990), Vol. 2, pp. 950 ff.
[3]T. Cselle and A. Barimani, Surf. Coat. Technol. **76–77**, 712 (1995).
[4]*Phase Diagrams of Ternary Boron Nitride and Silicon Nitride Systems*, edited by P. Rogl and J. C. Schuster (ASM International, Metals Park, OH, 1992).
[5]J. S. Koehler, Phys. Rev. B **2**, 547 (1970).
[6]S. Vepřek, M. Haussmann, S. Reiprich, L. Shizhi, and J. Dian, Surf. Coat. Technol. **86–87**, 394 (1996).
[7]D. Tabor, *The Hardness of Metals* (Clarendon, Oxford, 1951).
[8]C.-M. Sung and M. Sung, Mater. Chem. Phys. **43**, 1 (1996).
[9]R. W. Hertzberg, *Deformation and Fracture Mechanics of Engineering Materials*, 3rd ed. (Wiley, New York, 1989).
[10]M. L. Cohen, Phys. Rev. B **32**, 7988 (1985).
[11]A. Y. Liu and M. L. Cohen, Science **245**, 841 (1989).
[12]M. L. Cohen, Solid State Commun. **92**, 45 (1994).
[13]M. L. Cohen, Mater. Sci. Eng., A **209**, 1 (1996).
[14]S. Vepřek, J. Weidemann, and F. Glatz, J. Vac. Sci. Technol. A **13**, 2914 (1995).
[15]Y. Zhang, Z. Zhou, and H. Li, Appl. Phys. Lett. **68**, 634 (1996).
[16]Y. Zhang (private communication, 1997).
[17]Y. Chen, L. Guo, and E. G. Wang, Mod. Phys. Lett. B **10**, 615 (1996).
[18]Y. Chen, L. Guo, and E. G. Wang, J. Phys.: Condens. Mater. **8**, 685 (1996).
[19]Y. Chen, L. Guo, and E. G. Wang, Philos. Mag. Lett. **75**, 155 (1997).
[20]D. J. Johnson, Y. Chen, Y. He, and R. H. Prince, Diamond Relat. Mater. **6**, 1799 (1997).
[21]E. C. Cutiongco, D. Li, Y.-W. Chung, and C. S. Bhatia, J. Tribol. **118**, 543 (1996).
[22]A. Khurshudov, K. Kato, and S. Daisuke, J. Vac. Sci. Technol. A **14**, 2935 (1996).
[23]X. Yun, R. C. Hsiao, and D. B. Bogy, IEEE Trans. Magn. **33**, 938 (1997).
[24]R. C. Hsiao, D. B. Bodgy, and C. S. Bhatia, IEEE Trans. Magn. **34**, 1720 (1998).
[25]R. D. Ott, T. W. Scharf, D. Yang, and J. A. Barnard, IEEE Trans. Magn. **34**, 1735 (1998).
[26]Y. K. Yap, S. Kida, T. Aoyama, Y. Mori, and T. Sasaki, Appl. Phys. Lett. **73**, 915 (1998).
[27]M. Y. Cheng and P. T. Murray, J. Vac. Sci. Technol. A **16**, 2093 (1998).
[28]Y. F. Lu, Z. M. Ren, W. D. Song, and D. S. H. Chan, J. Appl. Phys. **84**, 2133 (1998).
[29]R. Soto, P. Gonzáles, X. Redondas, E. G. Parada, J. Pou, B. León, M. Pérez-Amor, M. F. da Silvia, and J. C. Soares, Nucl. Instrum. Methods Phys. Res. B **136–138**, 236 (1998).
[30]I. N. Mihailescu, E. Gyorgy, R. Alexandrescu, A. Luches, A. Perrone, C. Ghica, J. Werckmann, I. Cojocaru, and V. Chumash, Thin Solid Films **323**, 72 (1998).
[31]X. Q. Meng, Z. H. Zhang, H. X. Guo, A. G. Li, and X. J. Fan, Solid State Commun. **107**, 75 (1998).
[32]O. Takai, Y. Taki, and T. Kitagawa, Thin Solid Films **317**, 380 (1998).
[33]E. Q. Xie, Y. F. Jin, Z. G. Wang, and D. Y. He, Nucl. Instrum. Methods Phys. Res. B **135**, 224 (1998).
[34]J. Hartmann, M. Schreck, T. Baur, H. Huber, W. Assmann, H. Schuler, B. Strizker, and B. Rauschenbach, Diamond Relat. Mater. **7**, 899 (1998).
[35]G. Dinescu, E. Aldea, G. Musa, M. C. M. van de Sanden, A. de Graaf, C. Ghica, M. Gartner, and A. Andrei, Thin Solid Films **325**, 123 (1998).
[36]H. Oechsner, J. Vac. Sci. Technol. A **16**, 1956 (1998).
[37]Y. K. Yap, S. Kida, T. Aoyama, Y. Mori, and T. Sasaki, Jpn. J. Appl. Phys., Part 2 **37**, L746 (1998).
[38]L. C. Chen, T. R. Lu, C. T. Kuo, D. M. Bushari, J. J. Wu, K. H. Chen, and T. M. Chen, Appl. Phys. Lett. **72**, 3449 (1998).
[39]C.-Y. Hsu and F.C.-N. Hong, Jpn. J. Appl. Phys., Part 2 **37**, L675 (1998).
[40]A. Czyzniewski, W. Precht, M. Pancielejko, P. Myslinski, and W. Walkowiak, Thin Solid Films **317**, 384 (1998).
[41]L. Nobili, P. L. Cavallotti, G. Coccia Lecis, G. De Ponti, and C. Lenardi, Thin Solid Films **317**, 359 (1998).
[42]S. Yoshida, T. Itoh, N. Takada, S. Nitta, and S. Nonomura, J. Non-Cryst. Solids **227–230**, 650 (1998).
[43]X.-A. Zhao, C. W. Omg, Y. C. Tsang, K. F. Chan, C. L. Choy, P. W. Chan, and R. W. M. Kwok, Thin Solid Films **322**, 245 (1998).
[44]A. Wei, D. Chen, N. Ke, S. Peng, and S. P. Wong, Thin Solid Films **323**, 217 (1998).
[45]N. Tsubouchi, Y. Horino, B. Enders, A. Chayahara, A. Kinomura, and K. Fujii, Mater. Chem. Phys. **54**, 325 (1998).
[46]J. M. Méndez, A. Gaona-Cuoto, E. Andrade, J. C. Pineda, E. P. Zavala, and S. Muhl, Nucl. Instrum. Methods Phys. Res. B **136–138**, 231 (1998).
[47]E. J. Chi, J. Y. Shim, D. J. Choi, and H. K. Baik, J. Vac. Sci. Technol. B **16**, 1219 (1998).
[48]S. S. Todorov, D. Marton, K. J. Boyd, A. H. Al-Bayati, and J. W. Rabalais, J. Vac. Sci. Technol. A **12**, 3192 (1994).
[49]D. Marton, K. J. Boyd, and W. Rabalais, Int. J. Mod. Phys. B **9**, 3527 (1995).
[50]S. C. De Vries, Diamond Relat. Mater. **4**, 1093 (1995).
[51]C.-Z. Wang, E.-G. Wang, and Q. Dai, J. Appl. Phys. **83**, 1975 (1998).
[52]C. Ronning, H. Feldermann, R. Merk, H. Hpfsäss, P. Rienke, and J.-U. Thiele, Phys. Rev. B **58**, 2207 (1998).
[53]B. L. Korsounskii and V. I. Pepekin, Russ. Chem. Rev. **66**, 901 (1997).

[54]D. He, F. Zhang, X. Zhang, M. Zhang, R. Liu, Y. Xu, and W. Wang, Sci. China, Ser. A **41**, 405 (1998).
[55]D. Li, E. Cutiongco, Y.-W. Chung, M.-S. Wong, and W. D. Sproul, Diamond Films Technol. **5**, 261 (1995).
[56]M. R. Wixom, J. Am. Ceram. Soc. **73**, 1973 (1990).
[57]H. Sjöström, S. Stafström, M. Boman, and J.-E. Sundgren, Phys. Rev. Lett. **75**, 1336 (1995); **76**, 2205 (1996).
[58]H. Sjöström, L. Hultman, J.-E. Sundgren, S. V. Hainsworth, T. F. Page, and G. S. A. M. Theunissen, J. Vac. Sci. Technol. A **14**, 56 (1996).
[59]W. T. Zheng, H. Sjöström, I. Ivanov, K. Z. Xing, E. Broitman, W. R. Salaneck, J. E. Greene, and J.-E. Sundgren, J. Vac. Sci. Technol. A **14**, 2695 (1996).
[60]E. Broitman, W. T. Zheng, H. Sjöström, I. Ivanov, J. E. Greene, and J.-E. Sundgren, Appl. Phys. Lett. **72**, 2532 (1998).
[61]N. Hellgren, M. P. Johansson, E. Broitman, L. Hultman, and J.-E. Sundgren, Phys. Rev. B **59**, 5162 (1999).
[62]Ch. Kittel, *Introduction in Solid State Physics* (Wiley, New York, 1971).
[63]E. Hornbogen and H. Warlimont, *Metallkunde* (Springer, Berlin, 1996).
[64]A. Kelly and N. H. MacMillan, *Strong Solids*, 3rd ed. (Clarendon, Oxford, 1986).
[65]K. G. Schmitt-Thomas, *Metallkunde für das Maschinenwesen* (Springer, Berlin, 1990), Vols. I and II.
[66]M. F. Doerner and W. D. Nix, J. Mater. Res. **1**, 601 (1986).
[67]H.-H. Behnke, Härteri Technische. Mitteilungen **48**, 3 (1993).
[68]P. Neumaier, Metalloberfläche **2**, 41 (1989).
[69]T. F. Page and S. V. Hainsworth, Surf. Coat. Technol. **61**, 201 (1993).
[70]G. M. Pharr, W. C. Oliver, and F. R. Brotzen, J. Mater. Res. **7**, 613 (1992); W. C. Oliver and G. M. Pharr *ibid.* **7**, 1564 (1992).
[71]G. M. Pharr, Mater. Sci. Eng., A **253**, 151 (1998).
[72]A. Niederhofer, P. Nesladek, and S. Vepřek (unpublished).
[73]D. A. Dietrich and B. Rother, Materialprüfung **37**, 9 (1995).
[74]S. Vepřek, in *Hard Ceramic Materials*, edited by R. Riedel (Wiley–VCH, Weinhein, in press).
[75]S. Vepřek, Thin Solid Films **317**, 449 (1998).
[76]S. Vepřek, A. Niederhofer, P. Nesladek, and F. Glatz, Electrochem. Soc. Proc. **97-25**, 317 (1997).
[77]S. Vepřek, P. Nesladek, A. Niederhofer, F. Glatz, M. Jilek, and M. Sima, Surf. Coat. Technol. **108/109**, 138 (1998).
[78]I. M. Hutchings, Tribol. Int. **31**, 5 (1998).
[79]K. Tanaka, J. Mater. Sci. **22**, 1501 (1987).
[80]C. B. Poton and R. D. Rawlings, Mater. Sci. Technol. **5**, 865 (1989).
[81]P. Chantikul, G. R. Anstis, B. R. Lawn, and D. B. Marshall, J. Am. Ceram. Soc. **64**, 533 (1981); **64**, 539 (1981).
[82]A. Niederhofer, K. Moto, P. Nesladek, and S.Vepřek, Phys. Rev. B (submitted).
[83]B. Rother and D. A. Dietrich, Phys. Status Solidi A **142**, 389 (1994).
[84]B. Rother, J. Mater. Sci. **30**, 5394 (1995).
[85]B. Rother, Mat. -wiss. u. Werkstofftech **26**, 477 (1995).
[86]B. Rother, Mat. -wiss. u. Werkstofftech. **27**, 487 (1996).
[87]K.-Th. Wilke and J. Bohm, *Kristallzüchtung* (Deutsch, Frankfurt/Main, 1988).
[88]N. N. Greenwood and A. Earnshaw, *Chemistry of the Elements* (Pergamon, Oxford, 1984) German Translation (VCH, Weinheim, 1990).
[89]K. Nassau, *Gemstone Enhancement*, 2nd ed. (Butterworth-Heineman, Oxford, 1994).
[90]G. B. Bokii, N. F. Kirova, and V. I. Nepsha, Sov. Phys. Dokl. **24**, 83 (1979).
[91]R. H. Wentorf, Chem. Eng. **68**, 177 (1961).
[92]L. Vel, G. Demazeau, and J. Etourneau, Mater. Sci. Eng., B **10**, 149 (1991).
[93]K. Albe, Phys. Rev. B **55**, 6203 (1997).
[94]J. E. Buttler and H. Windischmann, MRS Bull. **23**, 22 (1998).
[95]W. G. Eversole, U.S. Patent Nos. 3,030,187 and 3,030,188 (1962).
[96]J. C. Angus, H. A. Will, and W. S. Stanko, J. Appl. Phys. **39**, 2915 (1968).
[97]D. J. Poferl, N. C. Gardner, and J. C. Angus, J. Appl. Phys. **44**, 1428 (1973).
[98]S. P. Chauhan, J. C. Angus, and N. C. Gardner, J. Appl. Phys. **47**, 4746 (1976).
[99]B. V. Deryagin, L. L. Builov, V. M. Zubkov, A. A. Kochergina, and D. V. Fedoseev, Sov. Phys. Crystallogr. **14**, 449 (1969).
[100]B. V. Deryagin and D. V. Fedoseev, Russ. Chem. Rev. **39**, 783 (1970).
[101]B. V. Deryagin and D. V. Fedoseev, Sci. Am. **233**, 102 (1975).
[102]H. Schmellenmeier, Exp. Tech. Phys. (Berlin) **1**, 49 (1953).
[103]H. Schmellenmeier, Z. Phys. Chem. (Leipzig) **205**, 349 (1956).
[104]S. Aeisenberg and R. Chabot, J. Appl. Phys. **42**, 2953 (1971).
[105]S. Aeisenberg and R. Chabot, J. Vac. Sci. Technol. **10**, 104 (1973).
[106]E. G. Spencer, P. H. Schmidt, P. H. Joy, and F. J. Sansalone, Appl. Phys. Lett. **29**, 118 (1976).
[107]V. E. Strelnitskii, I. I. Aksenov, S. I. Vakula, and V.G. Padakula, Sov. Phys. Tech. Phys. **23**, 222 (1978).
[108]P. Bachmann, D. Leers, and H. Lydtin, Diamond Relat. Mater. **1**, 1 (1991).
[109]D. M. Gruen, MRS Bull. **23**, 32 (1998).
[110]A. R. Patel and K. A. Cherian, Indian J. Pure Appl. Phys. **19**, 803 (1981).
[111]MRS Bull. **23**, 16 (1998).
[112]T. Yoshida, Diamond Relat. Mater. **5**, 501 (1996).
[113]S. Ulrich, J. Scherer, J. Schwan, I. Barzen, K. Jung, and H. Erhard, Diamond Relat. Mater. **4**, 288 (1995).
[114]M. Sueda, T. Kobayashi, T. Rokkaku, M. Ogawa, T. Watanabe, and S. Morimoto, J. Vac. Sci. Technol. A **16**, 3287 (1998).
[115]L. Holland and S. M. Ojha, Thin Solid Films **38**, L17 (1976).
[116]S. M. Ojha and L. Holland, Thin Solid Films **40**, L31 (1977).
[117]S. M. Ojha and L. Holland, Proceedings of the 7th International Vacuum Congress and 3rd International Conference on Solid Surfaces, Vienna, 1977, edited by R. Dobrozemsky, F. Rüdenauer, F. P. Viehböck, and A. Breth (F. Berger & Söhue, Horu, Austria, 1997), p. 1667.
[118]L. P. Anderson and S. Berg, Vacuum **28**, 449 (1978).
[119]S. Berg and L. P. Anderson, Thin Solid Films **58**, 117 (1979).
[120]T. J. Moravec, Thin Solid Films **70**, L9 (1980).
[121]K. Enke, H. Dimigen, and H. Hubsch, Appl. Phys. Lett. **36**, 291 (1980).
[122]C. Weissmantel, Thin Solid Films **58**, 101 (1979).
[123]C. Weissmantel, J. Vac. Sci. Technol. **18**, 179 (1981).
[124]A. Bubenzer, B. Dischler, G. Brandt, and P. Koidl, J. Appl. Phys. **54**, 4590 (1983).
[125]B. Dischler, A. Bubenzer, and P. Koidl, Appl. Phys. Lett. **42**, 636 (1983).
[126]J. Robertson, Pure Appl. Chem. **66**, 1789 (1994).
[127]J. Robertson, Diamond Relat. Mater. **3**, 361 (1994).
[128]A. A. Voevodin and M. S. Donley, Surf. Coat. Technol. **82**, 199 (1996).
[129]W. Jacobs, Thin Solid Films **326**, 1 (1998).
[130]F. Falk, J. Meinschien, K. Schuster, and H. Stafast, Carbon **36**, 765 (1998).
[131]A. R. Badzian, T. Niemyski, and E. Olkusnik, in Proceedings of the 3rd International Conference on Chemical Vapor Deposition, (Salt Lake City, April 1972), edited by F. A. Galski, p. 747.
[132]A. R. Badzian, MRS Bull. **16**, 1385 (1981).
[133]K. Montasser, S. Hattori, and S. Morita, Thin Solid Films **117**, 311 (1984).
[134]K. Montasser, S. Morita, and S. Hattori, Mater. Sci. Forum **54/55**, 295 (1990).
[135]R. A. Levy, E. Mastromatteo, J. M. Grow, V. Patari, and V. P. Kuo, J. Mater. Res. **10**, 320 (1995).
[136]T. M. Besmann, J. Am. Ceram. Soc. **73**, 2498 (1990).
[137]J. Löffler, F. Steinbach, J. Bill, J. Mayer, and F. Aldinger, Z. Metallkd. **87**, 170 (1996).
[138]D. Hegemann, R. Riedel, W. Dressler, C. Oehr, B. Schindler, and H. Brunner, Adv. Mater. Chem. Vap. Deposition **3**, 257 (1997).
[139]D. Hegemann, R. Riedel, and C. Oehr, Thin Solid Films **331**, 154 (1999).
[140]D. Hegemann, R. Riedel, and C. Oehr, Adv. Mater., Chem. Vap. Deposition **5**, 61 (1999).
[141]N. N. Sirota, M. M. Zhuk, A. M. Mazurenko, and A. I. Olekhnovich, Vesti. Adak. Nauk BSSR, Ser. Fiz.-Mat. Nauk **2** , 111 (1977); Chem. Abstr. **87**, 59009j (1977).
[142]A. K. Butylenko, G. V. Samsonov, I. I. Timofeeva, and G. Makarenko, Pis'ma Zh. Tekh. Fiz. **3**, 186 (1977); Chem. Abstr. **86**, 175831z (1977).
[143]S. Vepřek and M. Jurcik-Rajman, *Proceedings of the 7th International Symposium on Plasma Chemistry*, edited by J. Timmermans (Eindohoven University of Technology Press, Eindhoven, 1985), p. 90.
[144]S. Vepřek, Plasma Chem. Plasma Process. **12**, 219 (1992).
[145]S. Ulrich, T. Theel, J. Schwan, and H. Erhardt, Surf. Coat. Technol. **97**, 45 (1997).
[146]R. Riedel, Adv. Mater. **4**, 759 (1992).
[147]G. Will and K. H. Kossobutzki, J. Less-Common Met. **47**, 43 (1976).
[148]A. Inoue, H. M. Kimura, K. Sasamori, and T. Matsumoto, Japan. Inst. Metals Mater. Trans. **35**, 85 (1994).

[149]W. Dressler and R. Riedel, Int. J. Refract. Met. Hard Mater. **15**, 13 (1997).
[150]A. Badzian, T. Badzian, W. D. Drawl, and R. Roy, Diamond Relat. Mater. **7**, 1519 (1998).
[151]O. Knotek, R. Breidenbach, F. Jungblut, and F. Löffler, Surf. Coat. Technol. **43/44**, 107 (1990).
[152]O. Knotek and F. Löffler, J. Hard Mater. **3**, 29 (1992).
[153]S. Vepřek, F.-A. Sarott, and Z. Iqbal, Phys. Rev. B **36**, 3344 (1987).
[154]H. Oettel, R. Wiedemann, and S. Preissler, Surf. Coat. Technol. **74/75**, 273 (1995).
[155]W. Herr and E. Broszeit, Surf. Coat. Technol. **97**, 335 (1997).
[156]A. R. Badzian, T. Badzian, and L. Pilione, Int. J. Refract. Met. Hard Mater. **9**, 92 (1990).
[157]A. R. Badzian, Appl. Phys. Lett. **53**, 2495 (1988).
[158]T. Y. Tsui, G. M. Pharr, W. C. Olivier, Y. W. Chung, E. C. Cutiongco, C. S. Bhatia, R. L. White, R. L. Rhoades, and S. M. Gorbatkin, Mater. Res. Soc. Symp. Proc. **356**, 767 (1995).
[159]H. Holleck, J. Vac. Sci. Technol. A **4**, 2661 (1986).
[160]J. M. Léger, J. Haines, M. Schmidt, J. P. Petitet, A. S. Fereira, and J. A. H. da Jornada, Nature (London) **383**, 401 (1996).
[161]J. M. Léger and B. Blanzat, J. Mater. Sci. Lett. **13**, 1688 (1994).
[162]J. Haines and J. M. Léger, Phys. Rev. B **48**, 13344 (1993).
[163]U. Lundin, L. Fast, L. Nordström, B. Johansson, J. M. Wills, and O. Eriksson, Phys. Rev. B **57**, 4979 (1998).
[164]E. O. Hall, Proc. Phys. Soc. London, Sect. **B64**, 747 (1951).
[165]N. J. Petch, J. Iron Steel Inst., London **174**, 25 (1953).
[166]A. Lasalmonie and J. L. Strudel, J. Mater. Sci. **21**, 1837 (1986).
[167]E. Arzt, Acta Mater. **46**, 5611 (1998).
[168]A. I. Gusev, Usp. Fiz. Nauk **41**, 49 (1998).
[169]E. M. Lehockey, G. Palumbo, K. T. Aust, U. Erb, and P. Lin, Scr. Mater. **39**, 341 (1998).
[170]N. Hansen, Metall. Trans. A **16**, 2167 (1985).
[171]U. F. Koks, Metall. Trans. A **1**, 1121 (1970).
[172]R. W. Siegel and G. E. Fougere, Mater. Res. Soc. Symp. Proc. **362**, 219 (1995).
[173]R. W. Siegel and G. E. Fougere, Nanostruct. Mater. **6**, 205 (1995).
[174]H. Hahn and K. A. Padmanabhan, Philos. Mag. B **76**, 559 (1997).
[175]S. Yip, Nature (London) **391**, 532 (1998).
[176]J. Schiotz, E. D. Di Tolla, and K. W. Jacobsen, Nature (London) **391**, 561 (1998).
[177]J. E. Carsley, J. Ning, W. W. Milligan, S. A. Hackney, and E. C. Aifantis, Nanostruct. Mater. **5**, 441 (1995).
[178]A. H. Chokshi, A. Rosen, J. Karch, and H. Gleiter, Scr. Metall. **23**, 1679 (1989).
[179]G. W. Nieman, J. R. Weertman, and R. W. Siegel, Scr. Metall. **23**, 2013 (1989).
[180]J. S. C. Jang and C. C. Koch, Scr. Metall. Mater. **24**, 1599 (1990).
[181]K. Lu, W. D. Wie, and J. T. Wang, Scr. Metall. Mater. **24**, 2319 (1990).
[182]G. W. Nieman, J. R. Weertman, and R. W. Siegel, Scr. Metall. Mater. **24**, 145 (1990).
[183]G. W. Nieman, J. R. Weertman, and R. W. Siegel, J. Mater. Res. **6**, 1012 (1991).
[184]G. E. Fougere, J. R. Weertman, R. W. Siegel, and S. Kim, Scr. Metall. Mater. **26**, 1879 (1992).
[185]R. Z. Valiev, F. Chmelik, F. Bordeaux, G. Kapelski, and B. Baudelet, Scr. Metall. Mater. **27**, 855 (1992).
[186]A. M. El-Sherik, U. Erb, G. Palumbo, and K. T. Aust, Scr. Metall. Mater. **27**, 1185 (1992).
[187]P. G. Sanders, C. J. Youngdahl, and J. R. Weertman, Mater. Sci. Eng., A **234**, 77 (1997).
[188]P. G. Sanders, J. A. Eastman, and J. R. Weertman, Acta Mater. **45**, 4019 (1997).
[189]C. J. Youngdahl, P. G. Sanders, J. A. Eastman, and J. R. Weertman, Scr. Mater. **37**, 809 (1997).
[190]P. G. Sanders, J. A. Eastman, and J. R. Weertman, Acta Mater. **46**, 4195 (1998).
[191]J. Musil and F. Regent, J. Vac. Sci. Technol. A **16**, 3301 (1998).
[192]M. F. Ashby, Acta Metall. **20**, 887 (1972).
[193]H. Lüthy, R. A. White, and O. D. Sherby, Mater. Sci. Eng. **39**, 211 (1979).
[194]F. A. Mohamed and T. G. Langdon, Metall. Trans. A **5**, 2339 (1974).
[195]J. Crampon and B. Escaig, J. Am. Ceram. Soc. **63**, 680 (1980).
[196]R. C. Gifkins, Metall. Trans. A **7**, 1225 (1976).
[197]J. W. Edington, Metall. Trans. A **13**, 703 (1982).
[198]S.C. Lim, Tribol. Int. **31**, 87 (1998).
[199]S. L. Lehoczky, J. Appl. Phys. **49**, 5479 (1978).
[200]S. L. Lehoczky, Phys. Rev. Lett. **41**, 1814 (1978).
[201]C. A. O. Henning, F. W. Boswell, and J. M. Cobert, Acta Metall. **23**, 193 (1975).
[202]R. F. Bunshah, R. Nimmagadda, H. J. Doerr, B. A. Movchan, N. I. Grechanuk, and E. V. Dabizha, Thin Solid Films **72**, 261 (1980).
[203]S. Menezes and D. P. Anderson, J. Electrochem. Soc. **137**, 440 (1990).
[204]U. Helmersson, S. Todorova, S. A. Barnett, J.-E. Sundgren, L. C. Markert, and J. E. Greene, J. Appl. Phys. **62**, 481 (1987).
[205]M. Shinn, L. Hultman, and S. A. Barnett, J. Mater. Res. **7**, 901 (1992).
[206]X. Chu, M. S. Wong, W. D. Sproul, S. L. Rohde, and S. A. Barnett, J. Vac. Sci. Technol. A **10**, 1604 (1992).
[207]M. Larsson, P. Hollman, P. Hedenqvist, S. Hogmark, U. Wahlström, and L. Hultman, Surf. Coat. Technol. **86/87**, 351 (1996).
[208]K. M. Hubbard, T. R. Jervis, P. B. Mirkarimi, and S. C. Barnett, J. Appl. Phys. **72**, 4466 (1992).
[209]P. B. Mirkarimi, L. Hultman, and S. A. Barnett, Appl. Phys. Lett. **57**, 2654 (1990).
[210]P. B. Mirkarimi, S. A. Barnett, K. M. Hubbard, T. R. Jervis, and L. Hultman, J. Mater. Res. **9**, 1456 (1994).
[211]J.-E. Sundgren, J. Birch, G. Hakansson, L. Hultman, and U. Helmersson, Thin Solid Films **193–194**, 818 (1990).
[212]K. K. Shih and D. B. Dove, Appl. Phys. Lett. **61**, 654 (1992).
[213]W. D. Sproul, J. Vac. Sci. Technol. A **12**, 1595 (1994).
[214]W. D. Sproul, Surf. Coat. Technol. **86/87**, 170 (1996).
[215]W. D. Sproul, Science **273**, 889 (1996).
[216]M. L. Wu, X. W. Lin, V. P. Dravid, Y. W. Chung, M. S. Wong, and W. D. Sproul, J. Vac. Sci. Technol. A **15**, 946 (1997).
[217]D. Li, X. Chu, S. C. Cheng, X. W. Lin, V. P. Dravid, Y. W. Chung, M. W. Wong, and W. D. Sproul, Appl. Phys. Lett. **67**, 203 (1995).
[218]D. Li, X. W. Lin, S. C. Cheng, V. P. Dravid, Y. W. Chung, M. S. Wong, and W. D. Sproul, Appl. Phys. Lett. **68**, 1211 (1996).
[219]Y.-W. Chung, Surf. Rev. Lett. **3**, 1597 (1996).
[220]H. Jensen, J. Sobota, and G. Sorensen, Surf. Coat. Technol. **94/95**, 174 (1997).
[221]H. Jensen, J. Sobota, and G. Sorensen, J. Vac. Sci. Technol. A **16**, 1880 (1998).
[222]S. A. Barnett, in *Physics of Thin Films*, Vol. 17 Mechanics and Dielectric Properties, edited by M. H. Francombe and J. L. Vossen (Academic, Boston, 1993), p. 2.
[223]P. M. Anderson and C. Li, Nanostruct. Mater. **5**, 349 (19995).
[224]J. E. Krzanowski, Scr. Metall. Mater. **25**, 1465 (1991).
[225]X. Chu and S. A. Barnett, J. Appl. Phys. **77**, 4403 (1995).
[226]A. Madan, X. Chu, and S. A. Barnett, Appl. Phys. Lett. **68**, 2198 (1996).
[227]A. Madan, P. Yashar, M. Shinn, and S. A. Barnett, Thin Solid Films **302**, 147 (1997).
[228]S. Barnett and A. Madan, Phys. World **11**, 45 (1998).
[229]A. Madan, Y.-Y. Wang, S. A. Barnett, C. Enrgström, H. Ljungcrantz, L. Hultman, and M. Grimsditch, J. Appl. Phys. **84**, 776 (1998).
[230]M. Setoyama, A. Nakayama, T. Yoshioka, T. Nomura, A. Shibata, M. Chudou, and H. Arimoto, Sumimoto Electr. Ind. **146**, 91 (1995) (in Japanese).
[231]M. Setoyama, A. Nakayama, M. Tanaka, N. Kitagawa, and T. Nomura, Surf. Coat. Technol. **86/87**, 225 (1996).
[232]L. Hultman, G. Håkansson, U. Wahlström, J.-E. Sundgren, I. Petrov, F. Abidi, and J. E. Greene, Thin Solid Films **205**, 153 (1991).
[233]I. Petrov, F. Adibi, J. E. Greene, L. Hultman, and J.-E. Sundgren, Appl. Phys. Lett. **63**, 36 (1993).
[234]F. Adibi, I. Petrov, J. E. Greene, L. Hultman, and J.-E. Sundgren, J. Appl. Phys. **73**, 8580 (1993).
[235]M. Stüber, V. Schier, and H. Holleck, Surf. Coat. Technol. **74–75**, 833 (1995).
[236]H. Holleck and V. Schier, Surf. Coat. Technol. **76–77**, 328 (1995).
[237]H. Holleck, Ch. Kühl, and H. Schulz, J. Vac. Sci. Technol. A **3**, 2345 (1985).
[238]H. Holleck and H. Schulz, Surf. Coat. Technol. **36**, 707 (1988).
[239]S. A. Barnett, TSM Annual Meeting, San Antonio, TX, February 1998 (private communication).
[240]T. L. Selinder, M. E. Sjöstrand, Ä. Östlund, M. Larsson, S. Hogmark, and P. Hedenqvist, *Proceedings of the 14th International Plansee Seminar*,

edited by G. Kneringer, P. Rödhammer, and P. Wilharditz (Plansee AG, Reutte, Austria, 1997), p. 44.
[241]S. Vepřek, S. Reiprich, and L. Shizhi, Appl. Phys. Lett. **66**, 2540 (1995).
[242]S. Vepřek and S. Reiprich, Thin Solid Films **268**, 64 (1996).
[243]S. Vepřek, M. Haussmann, and S. Reiprich, J. Vac. Sci. Technol. A **14**, 46 (1996).
[244]S. Vepřek, M. Haussmann, and L. Shizhi, Electrochemical Soc. Proc. **96-5**, 619 (1996).
[245]S. Vepřek, S. Christiansen, M. Albrecht, and H. P. Strunk, Mater. Res. Soc. Symp. Proc. **457**, 407 (1997).
[246]S. Christiansen, M. Albrecht, H. P. Strunk, and S. Vepřek, J. Vac. Sci. Technol. B **16**, 19 (1998).
[247]S. Vepřek, M. Haussmann, and S. Reiprich, Mater. Res. Soc. Symp. Proc. **400**, 261 (1996).
[248]S. Vepřek, Thin Solid Films **297**, 145 (1997).
[249]W. W. Milligan, S. A. Hackney, M. Ke, and E. C. Aifantis, Nanostruct. Mater. **2**, 267 (1993).
[250]H. Tan and W. Yang, Mech. Mater. **30**, 111 (1998).
[251]G. W. Samsonow, *Nitridi* (Naukova Dumka, Kiev, 1969) (in Russian).
[252]H. Fischmeister and H. Jehn, *Hartstoffschichten zur Verschleissminderung* (DGM Informationsgesellschaft, Stuttgart, 1987).
[253]S. Sambasivan and W. T. Petuskey, J. Mater. Res. **9**, 2362 (1994).
[254]*JANAF Thermochemical Tables*, 3rd ed., edited by M. W. Chase, C. A. Davies, J. R. Downey, D. J. Fruip, R. A. McDonald, and A. N. Syverud, J. Phys. Chem. Ref. Data **14** (1985).
[255]T. Hirai and S. Hayashi, J. Mater. Sci. **17**, 1320 (1982); **17**, 3336 (1982); **18**, 2401 (1983).
[256]For the TiN/$Si_3N_4$, similar thermodynamic calculations were also done by A. G. Dias, J. H. Breda, P. Moretto, and J. Ordelman, J. Phys. IV, **2**, C5 (1995). However, the reported hardness was similar to that of TiN, presumably due to the high content of about 66 mol % $Si_3N_4$ (cf. Refs. 210 and 211).
[257]T. P. Mollart, J. Haupt, R. Gilmore, and W. Gissler, Surf. Coat. Technol. **86/87**, 231 (1996).
[258]P. Holubar, M. Jilek, and M. Sima, 26th International Conference on Metallurgical Coatings and Thin Films, San Diego, April 1999, Surf. Coat. Technol. (in press).
[259]L. Shizhi, S. Yulong, and P. Hongrui, Plasma Chem. Plasma Process. **12**, 287 (1992).
[260]SHM Ltd. Company, Masarykovo Nam. 3, CZ-78701 Sumperk, Czech Republic.
[261]M. Diserens, J. Patscheider, and F. Lévy, Surf. Coat. Technol. **108/109**, 241 (1998).
[262]S. Vepřek, P. Nesladek, A. Niederhofer, H. Männling, and M. Jilek, *Surface Engineering: Science and Technology I*, edited by A. Kumar, Y.-W. Chung, J. J. Moore, and J. E. Smugeresky (The Minerals, Metals & Materials Society, 1999), p. 219.
[263]A. Niederhofer, P. Nesladek, H.-D. Männing, S. Vepřek, and M. Jilek, International Conference on Metallic Coatings and Thin Films, San Diego, April 1999, Surf. Coatings Technol. (in press).
[264]A. von Engel, *Ionized Gases*, 2nd ed. (Clarendon, Oxford, 1965).
[265]S. C. Brown, *Introduction to Electrical Discharges in Gases* (Wiley, New York, 1966).
[266]G. Francis, *Ionization Phenomenon in Gases* (Butterworth, London, 1960).
[267]S. Vepřek, J. Th. Elmer, Ch. Eckmann, and M. Jurcik-Rajman, J. Electrochem. Soc. **136**, 2398 (1987).
[268]S. Vepřek, Ch. Eckmann, and J. Th. Elmer, Plasma Chem. Plasma Process. **8**, 445 (1988).
[269]T. Arai, H. Fujita, and K. Oguri, Thin Solid Films **165**, 139 (1988).
[270]D. Hoon, J. J. S. Chun, and J. G. Kim, J. Vac. Sci. Technol. A **7**, 31 (1989).
[271]J. Patscheider, L. Shizhi, and S. Vepřek, Plasma Chem. Plasma Process. **16**, 341 (1996).
[272]S. Vepřek, C. Brendel, and H. Schäfer, J. Cryst. Growth **9**, 266 (1971).
[273]O. Knotek, M. Böhmer, and T. Leyendecker, J. Vac. Sci. Technol. A **4**, 2695 (1986).
[274]T. Leyendecker, O. Lemmer, S. Esser, and J. Ebberink, Surf. Coat. Technol. **48**, 175 (1991).
[275]Y. Tanaka, T. M. Gür, M. Kelly, S. B. Hagstrom, T. Ikeda, K. Wakihira, and H. Satoh, J. Vac. Sci. Technol. A **10**, 1749 (1992).
[276]O. Knotek, A. Schrey, J. W. Schultze, and B. Siemensmeyer, Werkst. Korros. **43**, 511 (1992).
[277]C. Mitterer, M. Rauter, and P. Röhdammer, Surf. Coat. Technol. **41**, 351 (1990).
[278]M. Tamura and H. Kubo, Surf. Coat. Technol. **54/55**, 255 (1992).
[279]W. Gissler, Surf. Coat. Technol. **68/69**, 556 (1994).
[280]P. Hammer, A. Steiner, R. Villa, M. Baker, P. N. Gibson, J. Haupt, and W. Gissler, Surf. Coat. Technol. **68/69**, 194 (1994).
[281]T. P. Mollart, M. Baker, J. Haupt, A. Steiner, P. Hammer, and W. Gissler, Surf. Coat. Technol. **74/75**, 491 (1995).
[282]P. Losbichler, C. Mitterer, P. N. Gibson, W. Gissler, F. Hofer, and P. Warbichler, Surf. Coat. Technol. **94/95**, 297 (1997).
[283]W. Gissler, M. A. Baker, J. Haupt, P. N. Gibson, R. Gilmore, and T. P. Mollart, Diamond Films Technol. **7**, 165 (1997).
[284]C. Mitterer, P. Losbichler, F. Hofer, P. Warbichler, P. N. Gibson, and W. Gisler, Vacuum **50**, 313 (1998).
[285]O. Knotek and A. Barimani, Thin Solid Films **174**, 51 (1989).
[286]R. A. Andrievski, I. A. Anisimova, and V. P. Anisimov, Thin Solid Films **205**, 171 (1991).
[287]R. A. Andrievski, J. Solid State Chem. **133**, 249 (1997).
[288]R. A. Andrievski, J. Mater. Sci. **32**, 4463 (1997).
[289]M. Jilek, P. Klapetek, and M. Sima, *Proceedings of the 14th International Seminar*, edited by G. Kneringer, P. Rödhammer, and P. Wilharitz (Plansee AG, Reute, 1997), p. 294.
[290]R. Zallen, *The Physics of Amorphous Solids* (Wiley, New York, 1983).
[291]H. Warlimont and H. P. Aubauer, Z. Metallkd. **64**, 484 (1973).
[292]H. P. Aubauer and H. Warlimont, Z. Metallkd. **65**, 297 (1974).
[293]H. Schmalzried, *Chemical Kinetics of Solids* (VCH, Weinheim 1995).
[294]H. Schmalzried, *Solid State Reactions* (Verlag Chemie, Weinheim, 1981).
[295]*Diffusion Phenomena in Thin Films and Microelectronic Materials*, edited by D. Gupta and P. S. Ho (Noyes, Park Ridge, NJ, 1988), p. 43.
[296]A. L. Greer, Appl. Surf. Sci. **86**, 329 (1995).
[297]A. L. Greer, in *Mechanical Properties and Deformation Behavior of Materials Having Ultra-Fine Microstructures*, edited by M. Nastasi, D. M. Parkin, and H. Gleiter (Kluwer Academic, Dordrecht, 1993), p. 53.
[298]H. W. Sheng, J. Xu, L. G. Yu, K. K. Sun, Z. Q. Hu, and K. Lu, J. Mater. Res. **11**, 2841 (1996).
[299]H. W. Sheng, G. Ren, L. M. Peng, Z. Q. Hu, and K. Lu, J. Mater. Res. **12**, 119 (1997).
[300]H. W. Sheng, K. Lu, and E. Ma, Nanostruct. Mater. **10**, 865 (1998).
[301]T. P. Mollart, J. Haupt, R. Gilmore, and W. Gissler, Surf. Coat. Technol. **86/87**, 231 (1996).
[302]L. E. Toth, *Transition Metal Carbides and Nitrides* (Academic, New York, 1971).
[303]A. F. Wells, *Structural Inorganic Chemistry* (Clarendon, Oxford, 1984).
[304]H. Holleck and M. Lahres, Mater. Sci. Eng., A **140**, 609 (1991).
[305]O. Knotek (private communication).
[306]A. A. Voevodin and J. S. Zabinski, J. Mater. Sci. **33**, 319 (1998).
[307]A. A. Voevodin and J. S. Zabinski, Diamond Relat. Mater. **7**, 463 (1998).
[308]A. P. Alivisatos, Science **271**, 933 (1996).
[309]F.-R. F. Fan and A. J. Bard, Science **277**, 1791 (1997).
[310]D. L. Feldheim and Ch. D. Keating, Chem. Soc. Rev. **27**, 1 (1998).
[311]L. Tsybeskov, MRS Bull. **23**, 33 (1998).